

Obscured Activity: AGN, Quasars, Starbursts and ULIGs observed by the Infrared Space Observatory *

Aprajita Verma (verma@mpe.mpg.de)

Max-Planck Institut für extraterrestrische Physik, Postfach 1312, D-85741 Garching, Germany.

Vassilis Charmandaris (vassilis@astro.cornell.edu)

Department of Astronomy, Cornell University, 106 Space Sciences Building, Ithaca, NY 14853. Chercheur Associé, Observatoire de Paris, F-75014, Paris, France. Now at the University of Crete, Department of Physics, GR-71003, Heraklion, Greece.

Ulrich Klaas (klaas@mpia-hd.mpg.de)

Max-Planck-Institut für Astronomie, Königstuhl 17, D-69117 Heidelberg, Germany.

Dieter Lutz (lutz@mpe.mpg.de)

Max-Planck Institut für extraterrestrische Physik, Postfach 1312, D-85741 Garching, Germany.

Martin Haas (haas@astro.ruhr-uni-bochum.de)

Astronomisches Institut, Ruhr-Universität, Universitätsstr. 150, D-44780 Bochum, Germany.

Abstract. Some of the most 'active' galaxies in the Universe are obscured by large quantities of dust and emit a substantial fraction of their bolometric luminosity in the infrared. Observations of these infrared luminous galaxies with the Infrared Space Observatory (*ISO*) have provided a relatively unabsorbed view to the sources fuelling this active emission. The improved sensitivity, spatial resolution and spectroscopic capability of *ISO* over its predecessor Infrared Astronomical Satellite (*IRAS*), has enabled significant advances in the understanding of the infrared properties of active galaxies. *ISO* surveyed a wide range of active galaxies which, in the context of this review, includes those powered by intense bursts of star-formation as well as those containing a dominant active galactic nucleus (AGN). Mid infrared imaging resolved for the first time the dust enshrouded nuclei in many nearby galaxies, while a new era in infrared spectroscopy was opened by probing a wealth of atomic, ionic and molecular lines as well as broad band features in the mid and far infrared. This was particularly useful since it resulted in the understanding of the power production, excitation and fuelling mechanisms in the nuclei of active galaxies including the intriguing but so far elusive ultraluminous infrared galaxies. Detailed studies of various classes of AGN and quasars greatly improved our understanding of the unification scenario. Far-infrared imaging and photometry also revealed the presence of a new very cold dust component in galaxies and furthered our knowledge of the far-infrared properties of faint starbursts, ULIGs and quasars. We summarise almost nine years of key results based upon *ISO* data spanning the full range of luminosity and type of active galaxies.

Keywords: Galaxies: active, Galaxies: starburst, Galaxies: Seyfert, Galaxies: quasars, Infrared: galaxies



© Manuscript - To be published by Springer in 2005.
Space Science Review ISO Special Issue.

Received: 4 November 2004 **Accepted:** 15 November 2004

1. Introduction

“Activity” is a common feature of galaxies that emit a large fraction of their energy in the infrared. Existing primarily in a state of quiescence, during certain periods of their evolution galaxies experience short-lived phases of extreme star formation and/or black hole activity. From early ground-based measurements (e.g. Low and Kleinmann, 1968; Kleinmann and Low 1970b, 1970a) to surveys performed by the Infrared Astronomical Satellite (*IRAS*, Beichman et al., 1988), many previously known active galaxies [e.g. optical- or radio-selected quasars, active galactic nuclei (AGN), and starbursts] were found to be as or more powerful in the infrared than in the visible. In addition, a new population of optically faint, infrared luminous galaxies (luminous infrared galaxies (LIGs, with $L_{IR} > 10^{11} L_{\odot}$) were discovered that emit most of their bolometric luminosity in the infrared (Houck et al., 1984). AGN and massive bursts of star formation are the only known mechanisms that are capable of generating such luminosities. However, without spectroscopic information of the obscured components, classifying the underlying power source has proved to be difficult. Furthermore, quantitatively assessing the contribution to the total power from the two possible mechanisms is non-trivial. It is known that dust is formed during the late stages of stellar evolution and it is destroyed by intense radiation fields and shocks. Consequently, a detailed understanding of the physical mechanisms responsible for the observed infrared emission is an essential first step into revealing the nature of the underlying exciting source. As a result, since the most ‘active’ regions in our Universe appear to be enshrouded in large quantities of gas and dust, addressing the aforementioned points would have serious consequences in estimating star formation and black hole activity in the Universe.

In a cosmological context, both the reported increase in the star formation density of the Universe for $0.1 \lesssim z \lesssim 2$ (e.g. Madau et al., 1996; Barger et al., 2000) and the high frequency of starbursts hosted in galaxies with disturbed morphologies or in interacting/merging systems, imply that starbursts play an important role in galaxy formation and evolution. In addition, black hole activity could be buried in any luminous infrared system. Ultraluminous infrared galaxies (ULIGs, $L_{IR} > 10^{12} L_{\odot}$) have been proposed to be an evolutionary stage in the

* Based on observations with ISO, an ESA project with instruments funded by ESA Member States (especially the PI countries: France, Germany, the Netherlands and the United Kingdom) and with the participation of ISAS and NASA.

life of a quasar and the local analogues of the $z > 2$ (sub-)mm population. Quantifying the amount of obscured activity at earlier times and its contribution to the infrared and X-ray backgrounds remain open issues requiring a sound understanding of the properties of local active galaxies.

Following on from the coarse, photometric legacy of *IRAS*, *ISO* provided the first means to investigate the physical conditions of local active galaxies in significant detail at wavelengths where the obscured, and often most active, regions could be probed. Equipped with imaging, photometric and spectroscopic capabilities, *ISO* surveyed a wide range of emission properties from broad-band spectral energy distributions (SEDs), through imaging, to detailed spectral analysis. We discuss the infrared emission properties of obscured active galaxies that *ISO* surveyed during its lifetime. In the context of this chapter, ‘active’ refers to both star formation and black hole activity and encompasses the range of non-normal galaxies: interacting/merging galaxies; starbursts; radio galaxies; AGN; quasars; low ionisation nebular emission regions (LINERs); and the full suite of LIGs - ULIGs and hyperluminous infrared galaxies (HyLIGs $> 10^{13} L_{\odot}$).

2. Activity manifest in the infrared

High energy UV (and visible) photons emanating from active regions can heat or excite environmental dust, located around active sites or distributed throughout the interstellar medium (ISM), resulting in re-radiation in the infrared. Grains ranging from the very small (radius $a \lesssim 10\text{nm}$) to the large ($a \sim 30\mu\text{m}$) contribute to emission over the 2.5-200 μm range. The type, size and distribution of dust grains together with the incident interstellar radiation field (ISRF) shape the observed spectral features and overall form of the SED which arise from both thermal and non-thermal processes. At long infrared wavelengths ($\lambda \gtrsim 25\mu\text{m}$), emission predominantly arises from grains that re-radiate in thermodynamic equilibrium. In young radio galaxies, thermal bremsstrahlung may also provide a contribution to the infrared continuum. Emission related to transient rather than steady-state heating of dust grain complexes can dominate the SEDs of some active galaxies giving rise to continua and features over 3-18 μm . Non-thermal components include the featureless far-infrared tail (increases with increasing wavelength) of the synchrotron radiation spectrum in strong radio galaxies.

2.1. INFRARED CONTINUA: THERMAL AND NON-THERMAL

The mid-infrared spectra of galaxies display two continua: a flat continuum for $\lambda \lesssim 5\mu\text{m}$ and, in some galaxies, an unrelated continuum for $\lambda \gtrsim 11\mu\text{m}$ (Helou et al., 2000). These continua are not produced by grains heated to thermal equilibrium by the radiation field but arise from the stochastic heating of small dust grains (amorphous silicates and graphites, $a \sim 0.01\text{-}0.1\mu\text{m}$) which are transiently heated by the absorption of a single photon (Sellgren, 1984; Beichman, 1987; Boulanger et al., 1998b; Draine and Li, 2001; Draine, 2003). A single photon with energy of only a few electron volts ($\lambda \lesssim 0.4\mu\text{m}$), is sufficient for the onset of infrared emission (Uchida et al., 1998).

The steeply rising (near-thermal) continuum longward of $11\mu\text{m}$, which is strong in some active galaxies (but weak in quiescent galaxies), is thought to originate from the excess transient heating of very small fluctuating dust grains (VSG, $a \leq 10\text{nm}$). This component appears to be a characteristic of intensely star forming regions (Desert et al., 1990; Verstraete et al., 1996; Cesarsky et al., 1996b; Laureijs et al., 1996). Under this transient heating regime, the mid-infrared continuum is directly proportional to the underlying radiation field over several orders of magnitude and varies with the conditions of the H II regions from which it originates (Boulanger et al., 1998a; Laurent et al., 2000; Förster Schreiber et al., 2004). For example, in the close vicinity of the dense starburst knots in the Antennae, this continuum is shifted to shorter mid-infrared wavelengths implying higher temperatures (Vigroux et al., 1996).

The $3\mu\text{m} < \lambda < 5\mu\text{m}$ continuum is likely to arise from a featureless fluctuating component (Helou et al., 2000). Although often weak in active galaxies, the direct stellar continuum can also contribute ($\lambda < 5\mu\text{m}$) and should be considered in careful spectral decomposition analysis. The strength of this component increases with decreasing wavelength and thus the transition between direct stellar to interstellar dust emission occurs within the near- to low-mid-infrared (Boselli et al., 1997; Boselli et al., 1998; Alonso-Herrero et al., 2001). The mid-infrared also includes the transition from the transient to the steady-state heating regime. The wavelength at which this transition occurs is determined by the incident radiation field above which grains of a certain size no longer suffer large temperature changes. Dust grains are heated by the general ISRF and attain a 'steady-state' where emission and absorption reach an equilibrium. The grain temperature at which this equilibrium occurs characterises the emission giving rise to a thermal black-body continuum. Qualitatively, the mid- to far-infrared continua of active galaxies are often approximated by a series of superposed

black-bodies, each originating from a body of dust heated to a characteristic temperature (Haas et al., 1998a; Ivison et al., 1998; Klaas et al., 2001; Bendo et al., 2003; Stevens et al., 2005). This approximation provides only an indication of typical temperatures and is not an accurate description of the complex heating of a variety of dust grains. More accurate descriptions are achieved by considering a multi-grain dust model and complex radiation fields using, for example, semi-empirical models (e.g. Dale et al., 2001a) or radiative transfer theory (e.g. Acosta-Pulido et al., 1996; Silva et al., 1998; Alexander et al., 1999a; Siebenmorgen et al., 1999b; Efstathiou et al., 2000; Verma et al., 2002; Farrah et al., 2003; Freudling et al., 2003; González-Alfonso et al., 2004; Siebenmorgen et al., 2004a). For sources that are spatially unresolved by the *ISO* instruments, SED decomposition (using one of the methods above) is the only means to investigate the underlying physical processes.

Some AGN-hosting galaxies display a relatively broad and flat (in νF_ν) hot continuum that dominates their mid-infrared SEDs. This emerges from grains in the putative torus that are heated up to the grain sublimation temperature ($T_{sub} \sim 1500\text{K}$) by the strong radiation field of the accretion disk of the central AGN. The ‘warm’ *IRAS* galaxy criterion $S_{60}/S_{25} > 0.2$ selects galaxies displaying this component which are mostly identified with AGN (de Grijp et al., 1985).

The extended wavelength range of *ISO* over *IRAS* enabled (a) the precise determination of the turnover in the far-infrared SEDs of active galaxies and (b) the identification of two dust components that comprise the far-infrared emission that are both associated with large grains in thermal equilibrium. The first (or ‘cold’) component represents dust surrounding star forming regions and thus its strength is directly related to the star formation rate (however see Sect. 4.5). While the SEDs of normal quiescent galaxies peak at $\sim 150\mu\text{m}$, the enhanced heating in actively star forming regions produces a strong far-infrared peak at $\sim 60\text{-}100\mu\text{m}$ that dominates the infrared SED and corresponds to dust heated to 30-60K (e.g. Calzetti et al., 2000; Dale et al., 2001a; Spinoglio et al., 2002). This component also enhances the mid-infrared continuum (e.g. see Figure 1 in Sanders and Mirabel, 1996). In AGN, the fractional contribution of this ‘cold’ far-infrared component can be weaker in comparison to the warmer mid-infrared component ($\lambda \sim 30\mu\text{m}$) than in starbursts, reflective of the intense heating power of the AGN. The second (‘very cold’ or ‘cirrus’) component is dust that is spatially more extended and is associated with the HI disk or the molecular halo (Trewella et al., 2000; Radovich et al., 2001; Stickel et al., 2004). Located far and, in some galaxies, shielded (Calzetti et al., 2000) from the intense emission from the central engine,

the extended component is heated by the ambient interstellar radiation field to temperatures of 10-20K, (Odenwald et al., 1998; Alton et al., 1998; Davies et al., 1999; Haas et al., 1998b; Haas, 1998; Trewella et al., 2000). These temperatures are consistent with the theoretically predicted heating/cooling of dust grains in thermal equilibrium by a diffuse radiation field. Both profile measurements for resolved sources and far-infrared-sub-mm SED analysis for more distant galaxies reveal that a very cold component is required to explain all the emission beyond $100\mu\text{m}$ (Rodríguez Espinosa et al., 1996; Radovich et al., 1999; Siebenmorgen et al., 1999a; Domingue et al., 1999; Calzetti et al., 2000; Haas et al., 2000a; Klaas et al., 2001; Pérez García and Rodríguez Espinosa, 2001; Haas et al., 2003). This component, that *IRAS* was insensitive to, may be a significant contributor to the far-infrared luminosity in some active galaxies (e.g. $\gtrsim 60\%$ in local starbursts Calzetti et al., 2000).

2.2. FEATURES

The advent of *ISO* spectroscopy enabled the first sensitive and high resolution mid- to far-infrared spectroscopic measurements of active galaxies providing a better understanding of the physical conditions within visually obscured regions of systems such as Circinus (Moorwood et al., 1996; Sturm et al., 2000), the starburst M82 (Sturm et al., 2000) and the Seyfert 2 NGC1068 (Lutz et al., 2000b). The full 2.5-200 μm spectra of these three galaxies are shown in Fig. 1, and display the richness of the infrared range and the differences between these active galaxy templates (Sturm et al., 2000). The composite source Circinus displays broad mid-infrared features, fine structure lines of low excitation, H-recombination lines and a thermal continuum that predominantly trace the starburst component are intermingled with the strong VSG and mid-infrared AGN continua and high excitation fine structure lines that are predominantly caused by the hard radiation field of an AGN. In addition, warm and cold molecular gas and warm atomic gas are probed by rotational lines of H_2 , molecular absorption features (e.g. OH, CH, XCN, and H_2O) and very low excitation ($\lesssim 13.6\text{eV}$) fine structure lines (e.g. [OI], [CII]), respectively.

2.2.1. Unidentified Infrared Bands

The mid-infrared spectra of many active galaxies are dominated by characteristic broad emission features, the most prominent of which are located at 3.3, 6.2, 7.7, 8.6 and $11.3\mu\text{m}$. They are invariably observed together and are commonly referred to as unidentified infrared bands (UIBs). These features have been detected in a wide range of celestial sources (e.g. Allamandola et al., 1995; Cesarsky et al., 1996a; Cesarsky

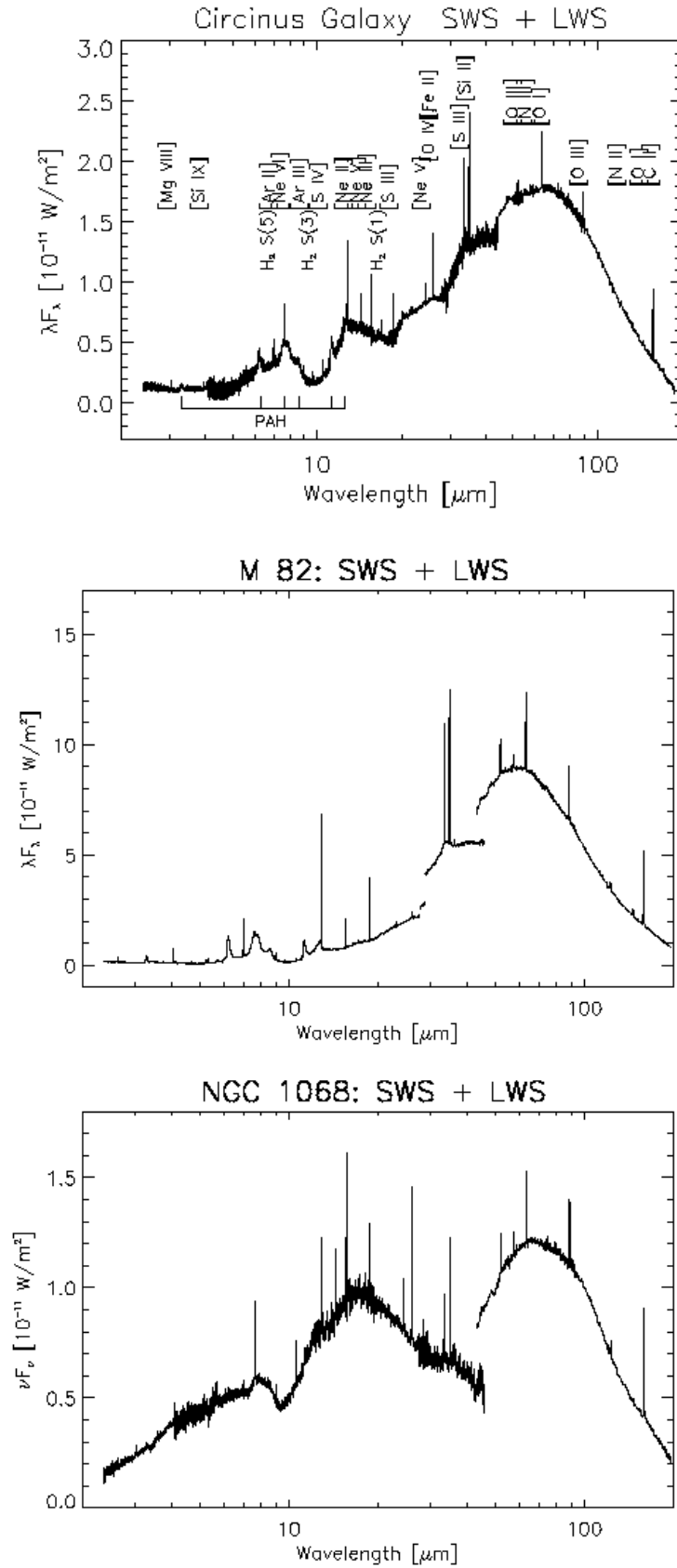


Figure 1. Composite SWS+LWS spectra of Circinus, M82 and NGC 1068 displaying the spectral differences between the different source types (Sturm priv. comm.).

et al., 1996b; Verstraete et al., 1996; Mattila et al., 1996; Lemke et al., 1998; Mattila et al., 1999) and are commonly detected in the spectra of normal galaxies. UIBs may originate from C-C and C-H bending and stretching vibrational modes in aromatic hydrocarbons (Leger and Puget, 1984; Allamandola et al., 1985; Puget and Leger, 1989) and the favoured carriers are polycyclic aromatic hydrocarbons (PAHs). The features are attributed to PAH clusters (Boulanger et al., 1998b), while individual PAHs can contribute to the 5-10 μ m continuum and may be responsible for the non-linear continuum rise seen in the far UV (Siebenmorgen and Kruegel, 1992). Alternative carriers are small amorphous carbon grains that emit when exposed to moderately intense UV/visible radiation (Puget and Leger, 1989; Boulade et al., 1996; Uchida et al., 1998; Pagani et al., 1999). Since the exact molecular structure of the carriers remains under debate, the features are referred to as UIBs throughout this text (for a more thorough review on the structure of UIBs see the chapter of Peeters et al. in this volume or Peeters et al. (2003)). Where strongly detected, the carriers are likely to provide the majority of the flux in the 3-12 μ m band and show near-invariant profiles in a variety of galaxies (Rigopoulou et al., 1999; Helou et al., 2000; Förster Schreiber et al., 2003). The widths of the lines are thought to arise from temperature broadening of the vibrational bands and have been fit using Lorentzian rather than Gaussian profiles (Boulanger et al., 1998b; Verstraete et al., 2001) but see the discussion in Peeters et al. (this volume) for further details on this issue. The spatial correlation between mid-infrared emission with atomic and molecular hydrogen suggests that UIB emission originates at the interface of H II and molecular clouds, the so-called photo-dissociation regions (PDRs, e.g. Verstraete et al., 1996; Cesarsky et al., 1996b; Pagani et al., 1999).

Mid-infrared starburst spectra are generally dominated by these UIB features and show a strong continuum from very small grains. The relative strengths of the features are sensitive to local radiation fields, distribution of grains throughout the galaxy system and extinction (Verstraete et al., 1996; Sturm et al., 2000; Lutz et al., 1998b; Laurent et al., 2000). UIB emission in starburst regions originates from UV-heated ionised UIB carriers. A significant contribution can also arise in heating of neutral UIB carriers in the extended regions by the diffuse ISRF i.e. by less energetic (visible) photons, which is mostly seen in normal galaxies and is proposed in some active galaxies (Mattila et al., 1999; Smith, 1998; Pagani et al., 1999; Haas et al., 2002).

In intense radiation fields ($\sim 10^5$ times that of the local ISRF) such as in metal poor environments or in the vicinity of super star clusters or AGN, UIBs are weak or absent (Contursi et al., 2000; Thuan

et al., 1999; Rigopoulou et al., 1999; Sturm et al., 2000; Santos-Lleó et al., 2001). Small grains and UIB carriers are susceptible to high temperature fluctuations and photons with sufficient energy may cause grain sublimation or destruction. This is reflected in the UIB-to-mid-infrared continuum strength ratio ($7\mu\text{m}/15\mu\text{m}$ flux density) that is seen to be lower (>0.5) in active regions and galaxies than in more quiescent regions such as in normal galaxies and the disks of some active galaxies [ratio ~ 1 with a large dispersion, see Fig. 1 of Vigroux et al. (1999) and Fig. 12 in Dale et al. (2000)]. Weak detections of UIBs in galaxies with AGN probably originate from the cooler material such as circumnuclear starburst regions or diffusely heated extended regions rather than from the immediate vicinity of the AGN torus. In nearby Seyferts, spatially resolved mid-infrared spectroscopy suggested that the absence or suppression of UIB emission is due to the fact that the dust is predominantly heated by processes related to the central AGN [e.g. in NGC 1068 (Le Floc’h et al., 2001), Circinus (Moorwood, 1999), NGC 4151 (Sturm et al., 1999), Mrk 279 (Santos-Lleó et al., 2001)]. This was confirmed through a comparison of *ISO* and high spatial resolution ground based data of AGN and starbursts, that demonstrated the absence of UIBs in the nuclei of AGN-hosting galaxies (Siebenmorgen et al., 2004b). For unresolved sources the VSG continuum may be so strong that the UIB features are diluted by the over-powering continuum resulting in their non-detection (Lutz et al., 1998b). Thus at high redshifts, where low-metallicity- and/or AGN-dominated- systems may be more prevalent, the intrinsic weakness of UIB features seen in local systems of these types would imply that the use of UIB features as a tracer of similar systems at high redshift may be problematic.

2.2.2. *Fine structure lines*

Fine structure lines are tracers of nebular conditions such as excitation and the intrinsic ionising spectrum. By virtue of their differing excitation potentials and critical densities they provide an insight into the energetics and chemical composition of the regions from which they originate. Starburst galaxies commonly show low excitation fine structure lines (e.g. [ArII], [ArIII], [FeII], [NeII] and [SIII]) that have ionisation potentials between 13.6eV and $\sim 50\text{eV}$ and mostly arise from H II regions that have been photoionized by their central massive stars. A PDR or shock origin may also contribute to the flux of some low-excitation lines. High excitation lines with potentials exceeding 50eV (e.g. [NeV,VI], [SIV],[MgV,VII,VIII] [OIV], [SiV,VI,VII]) are present in the spectra some low-metallicity galaxies but are more commonly found in AGN where high energy photons, produced by non-thermal processes related to the central black hole, photoionise the gas. Ex-

citation to these high energy levels ($>50\text{eV}$) is difficult to attain by photons emitted by stars in typical HII regions. However, the mid-infrared spectra of some starbursts do show the high excitation [OIV] and [SIV] lines. The presence of these lines is associated to collisionally excited, shocked or coronal gas (e.g. Lutz et al. (1998a)). Active galaxy spectra also show fine structure lines with excitation potentials below the ionisation potential of hydrogen (e.g. [OIII]52,88 μm , [OI]63,145 μm and [CII]158 μm), that trace mostly cool atomic and molecular clouds. [CII]158 μm and [OI]63 μm are important cooling lines in PDRs but also originate in widespread atomic gas (see section 4.6).

As infrared fine structure lines are fairly insensitive to uncertainties of the effective temperature of the gas, and because they are less affected by extinction than optical lines, they provide an unequalled insight into the properties of the ISM (e.g. electron temperature and density, ISRF, metallicity) of active galaxies and their embedded power source. Ratios of two lines of the same species provide information on the nebular conditions such as electron temperatures and densities. Ratios of high to low excitation states of the same element probe the hardness of the ISRF and ratios of high- to low-excitation lines of different elements have been used as tracers of AGN presence and thus contribute to nebular diagnostics (see section 6.1). Spectroscopic data from *ISO* was a major advance over *IRAS* enabling the quantitative estimation of the dominant fuelling mechanism in a given source (Genzel et al., 1998; Laurent et al., 2000; Sturm et al., 2000).

2.2.3. *Molecular Features*

Molecular features trace the cold dense molecular material in active galaxies. Several active gas-rich starbursts, Seyferts and ULIGs display a range of molecular lines: the rotational lines of molecular hydrogen (Sect. 2.2.3.2), OH, H₂O, NH₃ and CH are seen in absorption or emission (see Fig. 1 of Fischer et al., 1999b, also refer to Hur et al., 1996; Fischer et al., 1997; Bradford et al., 1999; Fischer et al., 1999a; Fischer et al., 1999b; Colbert et al., 1999; Sturm et al., 2000; Rigopoulou et al., 2002; Spoon et al., 2002; Spinoglio et al., 2005). Molecular absorption features appear to be more common (and prominent) in sources of high luminosity (e.g. ULIGs) than those of lower luminosity (Fischer et al., 1999b; Fischer et al., 1999a; Spoon et al., 2002). Spectra displaying molecular absorption features show a wide variety of excitation: from starburst galaxies like M82 which display features indicating that most of the O and C molecules occupy the ground-state, to objects such as ULIGs where a significant population exists at higher energy levels (Fischer et al., 1999b; Fischer et al., 1999a). Additional absorption features at 6.85 and 7.25 μm are seen in the spectra of some active galaxies and

ULIGs (Spoon et al., 2002). They are attributed to CH-deformation modes of carbonaceous material because of their similarity to features seen along lines of sight towards Sgr A* (Chiar et al., 2000). ULIG and Seyfert spectra also exhibit an absorption feature at $3.4\mu\text{m}$ that is likely to be aliphatic CH stretch absorptions of refractory carbonaceous material (Imanishi, 2002; Dartois et al., 2004).

2.2.3.1. Silicate Absorption The $9.7\mu\text{m}$ and $18\mu\text{m}$ absorption features arise from the stretching and bending modes of SiO. The extinction suffered by a galaxy can be estimated by the depth of these lines. For example, the extreme $9.7\mu\text{m}$ silicate absorption feature seen in the starburst-ULIG Arp 220 provides a lower limit to the optical depth of $A_V \gtrsim 45$ (Charmandaris et al. (1997), but see Spoon et al. (2004) for a more detailed analysis of this system). Though it is possible that the depth of the $9.7\mu\text{m}$ may be overestimated in the feature-dense mid-infrared spectra of starbursts exhibiting UIB emission, (Sturm et al., 2000; Förster Schreiber et al., 2003). The extreme extinction of the starburst M82 ($A_V = 15-60$) derived by Gillett et al. (1975) was ascribed to this problem as *ISO* data could not support such a high extinction (Sturm et al., 2000).

2.2.3.2. Molecular hydrogen and warm molecular gas Rotational transitions of H_2 that originate in dense molecular media were detected in the spectra of several active galaxies: NGC 3256 (Rigopoulou et al., 1996); NGC 891 (Valentijn and van der Werf, 1999); NGC 1068 (Lutz et al., 2000b); NGC 4945 (Spoon et al., 2000); NGC 6240 (Lutz et al., 2003). Low rotational transitions originate from warm gas ($T \sim 100-200\text{K}$) and the higher and rovibrational lines from much hotter gas ($T \gtrsim 1000\text{K}$). Rigopoulou et al. (2002) investigated a sample of starbursts and Seyferts observed by *ISO* presenting pure rotational lines from S(7) to S(0). Irrespective of starburst or Seyfert type, temperatures of $\sim 150\text{K}$ are derived from the S(1)/S(0) ratio. A similar temperature was found for NGC 4945 (Spoon et al., 2000). While $\sim 10\%$ of the galactic gas mass in a starburst system can be accounted for by the warm component, on average higher fraction (18%, range 2-35%) are observed for Seyferts (Rigopoulou et al., 2002). The temperature of the molecular hydrogen implies that it arises from a combination of emission from fairly normal PDRs (at least for starbursts), low velocity shocks and X-ray heated gas around the central AGN. The latter is more probable in Seyfert galaxies which accounts for the larger fraction of warm gas found in these systems. Shock heating appears to be the most likely origin of the extremely strong rotational H_2 lines detected in the merging ‘double active nucleus’ system NGC 6240 (Lutz et al.,

2003). While, the origin of shock-heating can be largely associated to winds originating from massive stars and supernovae, recently Haas et al. (2005) have found the first observational evidence of pre-starburst shocks in the overlap region of the early merger the Antennae (see Section 4.1). From a re-analysis of archival *ISOCAM-CVF* data, they find that the strongest molecular hydrogen emission (traced by the $\text{H}_2\text{S}(3)$ line) is displaced from the regions of active star formation. This, together with the high line luminosity (normalised to the far-infrared luminosity) indicates that the bulk of excited H_2 gas is shocked by the collision itself.

2.2.3.3. Ice absorption and cold molecular gas An interesting discovery made by *ISO* was the first extragalactic detection of absorption features due to ices (H_2O , CH_4 and XCN) present in cold molecular components of starbursts, Seyferts and predominantly ULIGs. Sturm et al. (2000) first reported the detections of weak water ice absorption features at $3\mu\text{m}$ in the spectra of local starbursts M 82 and NGC 253. Very strong water ice, as well as the first detections of absorptions due to CO and CO_2 ices, were detected in the actively star-forming galaxy NGC 4945 (Spoon et al., 2000). The presence of ices is related to the presence of cold material and the radiation environment. One would expect cold molecular clouds in starbursts to be likely hosts while more intense environments, such as those predominantly fuelled by AGN, to be less favoured. This is corroborated by the lack of absorption features in the spectrum of NGC 1068 (Sturm et al., 2000) and the limits on the strength of the CO absorption feature set from *ISOSWS* spectra of 31 AGN (Lutz et al., 2004b). However, water ice absorption has been detected in Seyfert galaxies, e.g. in the UIB-free spectrum of the Seyfert galaxy NGC 4418 (Spoon et al., 2001). The absorption dominated spectrum bears strong similarities to the spectra of embedded protostars, and the depth of absorption features implies that its Seyfert nucleus is so deeply embedded that ices are shielded from the intense radiation field of the AGN.

In a heterogeneous sample of 103 active galaxies with high signal-to-noise mid-infrared spectra, approximately 20% display absorption features attributed to ices (Spoon et al., 2002). While ices are weak or absent in the spectra of starbursts and Seyferts, in ULIGs they are strong, considerably stronger than the weak features found previously in M 82 and NGC 253. This implies that rather than the radiation environment it is the amount of cold material that determines their presence in these most luminous and massive infrared galaxies that are known to contain large concentrations of molecular material (e.g. Solomon et al. (1997); Downes and Solomon (1998)). Although plausible, more

sensitive (and spatially resolved) mid-infrared spectroscopy is required to understand these differences, and the distribution and energetic conditions of cold molecular material. Moreover, higher spectral resolution over a wider mid-infrared wavelength range is necessary for accurate decomposition of the spectra into their various components, which will aid identification of subtle and/or blended features (e.g. Spoon et al., 2004). Spoon et al. (2002) proposed an evolutionary sequence for their ice spectra ranging from a highly obscured beginning of star formation where ices dominate the spectra, to a less obscured stage of star formation where the UIBs become stronger. At any stage the star formation may be accompanied by AGN activity.

2.2.3.4. OH features and (Mega-)masers Transitions of the OH molecule were also detected in the *ISOSWS* and *ISOLWS* spectra of some active galaxies (Fischer et al., 1999b), such as in the starbursts NGC 253 (Bradford et al., 1999) and NGC 4945 (Brauhar et al., 1997) permitting estimation of the OH column density and abundance. The depths of the OH features detected in the *ISOLWS* far-infrared spectra of galaxies hosting known OH (mega-)masers were found to be sufficient to provide all of the infrared photons required to radiatively pump the maser activity (e.g. in the starburst-ULIG Arp 220 (Skinner et al., 1997; Suter et al., 1998); AGN-ULIG Mrk 231 (Suter et al., 1998); the merging double systems ULIG IRAS 20100-4156 and LIG 3 Zw 35 (Kegel et al., 1999); the starburst NGC 4945 (Brauhar et al., 1997)). In Arp220, the fact that the far-infrared continuum source is extended and that the maser must be located in front of it favours the interpretation that a starburst provides the continuum photons for its maser (Skinner et al., 1997). The high pump rate determined for this source suggests that pumping mechanisms other than radiative pumping (such as collisional pumping) may contribute (He and Chen, 2004).

2.3. MAGNETICALLY ALIGNED DUST GRAINS

Polarised emission detected from active galaxies is ascribed to dichroic absorption by the ISM of a galaxy i.e. by elongated dust grains that are magnetically aligned. This has been observed in galactic sources where the position angle of the measured polarisation indicates the orientation of the projected magnetic field. Polarisation is an important probe of the physical conditions in active galaxies as it can provide constraints on the formation of the putative torus (Alexander et al., 1999b). Such polarisation studies were performed for some ULIGs and revealed 3-8% of the 5-18 μ m flux to be polarised (Siebenmorgen and Efstathiou, 2001). The archetypal starburst-like ULIG Arp220 has the

lowest polarisation while the warm AGN-like Mrk 231 ULIG the highest. The first polarisation profile of a starburst galaxy was made at $6\mu\text{m}$ for NGC 1808 showing a 20% increase towards the outer regions (Siebenmorgen et al., 2001). This, together with a complementary measurement at $170\mu\text{m}$ (unresolved), are best explained by the large scale ($\sim 500\text{pc}$) magnetic alignment of (non-spherical) large grains ($\geq 100\text{\AA}$).

3. Very Cold dust and diffuse radiation fields: ISM

ISOPHOT-data clearly confirmed the presence of very cold dust ($T\sim 10\text{--}20\text{K}$) in a variety of infrared galaxies. Often in conjunction with supplementary (sub-)mm photometry, this component was detected in spatially resolved maps or intensity profiles of local galaxies (e.g. Haas et al. (1998b)), and was isolated as a significant contributor to the far-infrared luminosity in SED analyses of unresolved active galaxies (Calzetti et al., 2000; Klaas et al., 2001; Spinoglio et al., 2002; Haas et al., 2003). Although cold 'cirrus' or 'disk' components in galaxies were indicated by *IRAS* colours, *IRAS* was insensitive to this very cold component due to its shorter wavelength coverage ($< 100\mu\text{m}$). As a result gas-to-dust ratios of distant galaxies based solely upon *IRAS* data were overestimated whereas the addition of *ISO* measurements resulted in values which are closer to that of the Galactic value (~ 160) (Haas et al., 1998b). The very-cold component often accounts for a substantial fraction of far-infrared emission and is most commonly seen in early type and disk galaxies (see Sauvage et al. this volume). With a scale-length in excess of the stars, less than the atomic HI gas and similar to that of the molecular gas, it is likely that the dust is associated to this cold gas components (e.g. Davies et al., 1999; Popescu and Tuffs, 2003; Popescu et al., 2004).

Very-cold dust is also seen in both starburst and AGN-hosting active galaxies. NGC 253, that hosts a nuclear starburst, has been shown to contain extended cold dust along the major and minor axes. While the dust along the minor axis is attributed to outflows, the cold emission along the major axis is shown to have a scale length 40% greater than that of the stars (Radovich et al., 2001). The correlation of the $90\mu\text{m}$ emission profile of four Seyfert galaxies with the R-band extent but not with the star formation tracer $\text{H}\alpha$ suggests that a large contribution of the far-infrared emission from Seyferts does not arise from the (nuclear) star-forming regions but from a cooler far-infrared disk component within which normal stars heat dust grains (Pérez García et al., 2000). The detection of substantial cold far-infrared emission ($T < 20\text{K}$) from the star-forming obscured overlap region of the merging

Antennae galaxy (see Section 4.1) indicates the presence of cold dense dust within which stars are forming (Haas et al., 2000a).

SED analysis using black or grey-body decomposition suggested the need for more than one dust component, including a very cold dust component, to explain the emission above $100\mu\text{m}$ of many galaxies. However, by allowing both temperature and dust grain emissivity to be free parameters, it is possible to approximate the entire far-infrared SED ($\lambda > 50\mu\text{m}$) using a single modified black body. Invariably for active galaxies this was achieved with temperatures $\sim 30\text{-}50\text{K}$ and emissivity values of 1.5-2 (e.g. Colbert et al., 1999; Siebenmorgen et al., 1999a). However, by doing so raised conflicts with other observational constraints (see Klaas et al. (2001) for a full description). Moreover by leaving the dust emissivity as a free parameter presupposes that intrinsic dust properties differ from source to source with no physical basis supporting this assumption. By choosing a Galactic value of $\gamma=2$ for the grain emissivity (i.e. assuming that dust properties do not vary between sources), single black-bodies fail to explain all the far-infrared emission - additional cold components ($T\sim 10\text{-}20\text{K}$) are required that are associated with the spatially resolved extended very cold components described above.

The SEDs of active galaxies are warmer than those of normal galaxies and the far-infrared part is generally fit by two components representing active star formation and very cold (diffusely heated) material. The very cold dust can be a significant contributor in terms of galaxy mass and energy output. For example, two of the three components used to fit the SED of the LINER NGC 3079 have very cold temperatures of 12 and 20K, respectively (Klaas and Walker, 2002). Calzetti et al. (2000) find that two dust components are required at $T=40\text{-}55\text{K}$ and $T\sim 20\text{-}23\text{K}$ to explain the far-infrared SEDs of eight local starbursts. The latter comprises up to 60% of the total flux and the associated mass is as much as 150 times that of the former. For the most actively star forming galaxies or those with strongest radiation fields, the contribution to the bolometric luminosity from cold emission (as measured in the $122\text{-}1100\mu\text{m}$ range) was shown to be smaller in actively star forming (5%) than in cirrus dominated galaxies ($\sim 40\%$) (Dale et al., 2001a). SED analysis of a wide range of active galaxies indicates that very cold components are common whether they are centrally fuelled by AGN or starbursts, suggesting that the central activity does not directly affect the far-infrared emission.

4. Cold dust and low excitation radiation fields: starburst regions

The T=40-45K temperature component found in local starbursts by Calzetti et al. (2000) mentioned above represents the emission from dust surrounding sites of active star formation. For starburst galaxies this emission (peaking between 60 and 100 μm) dominates the infrared SED and is the major contributor to the infrared luminosity. This 'cold' infrared emission is generally less extended than the very cold component described in the preceding section. In some nearby galaxies, the far-infrared morphology traces star forming regions well. For example, the strongly far-infrared-emitting dark molecular cloud coincides with a cluster of star forming regions in the galaxy NGC 4051 (Pérez García et al., 2000). Similarly, far-infrared emission could be resolved for the pair members of interacting spirals where enhanced star formation has been established (Xu et al., 2000; Gao et al., 2001). The correlation of the warmer far-infrared emission with the R-band morphology of local Seyferts hosting compact nuclei and circumnuclear star formation further supports that this far-infrared component is related to star formation activity (Rodríguez Espinosa and Perez Garcia, 1997). Moreover, far-infrared emission has also been spatially associated with regions exhibiting signs of strong star formation (e.g. strong UIBs). Roussel et al. (2001) demonstrated that the integrated far-infrared flux and the star-formation related mid-infrared flux are strongly correlated in the disks of normal star forming galaxies indicating that the grains responsible for the mid- and far-infrared share a common heating source.

4.1. THE IMPORTANCE OF INTERACTIONS/MERGERS

Interactions and mergers enhance starburst activity, both nuclear and extra-nuclear (see review by Struck, 1999). The final merger stage plays a critical role in how active galaxies form stars and may influence the appearance of AGN and the onset of the ULIG phase. The fraction of disturbed or interacting systems in infrared selected samples of galaxies appears to increase with luminosity with nearly 100% of all ULIGs displaying evidence of interaction (see Sanders and Mirabel, 1996 and references therein). Numerical simulations have also helped in establishing that interactions and mergers play an important role in the formation and evolution of such galaxies (Mihos and Hernquist, 1996). The induced gravitational instabilities form bars which strip in-falling gas of angular momentum and enable radial inflows to the nuclear regions that can feed starbursts or AGN (Combes, 2001). Moreover,

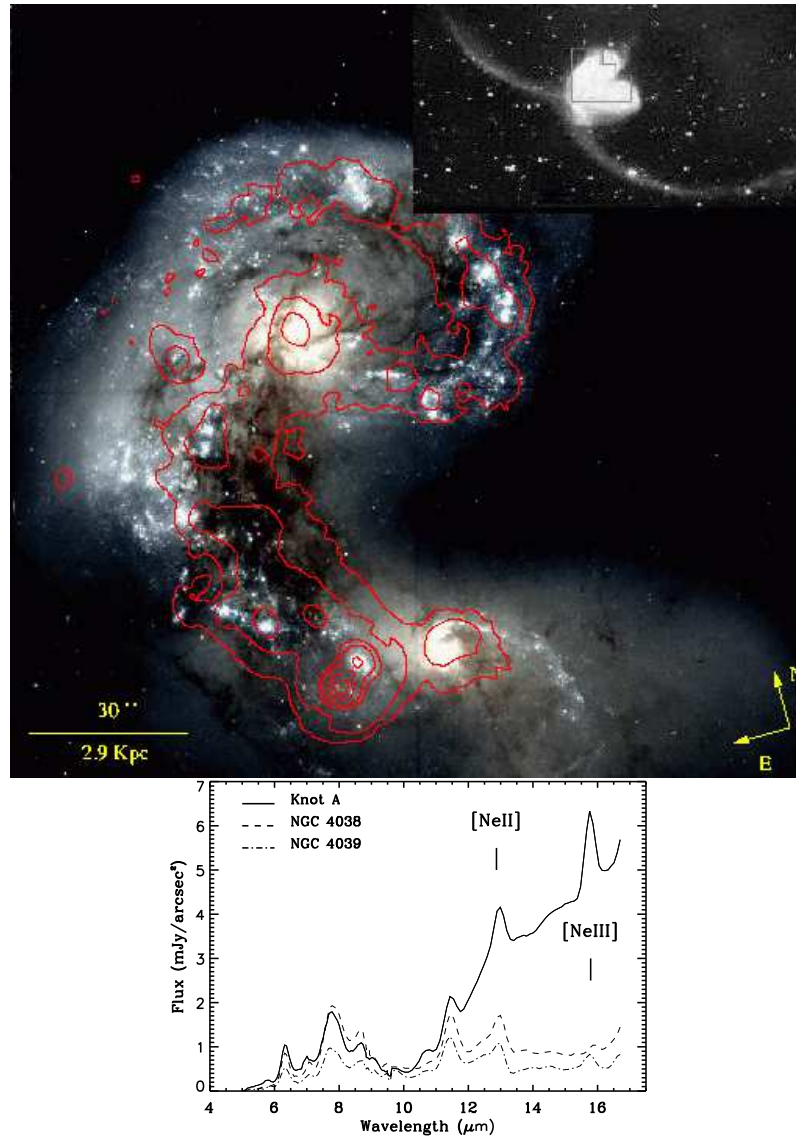


Figure 2. This composite figure of the Antennae is from Mirabel et al. (1998) showing the *ISOCAM*-CVF contours overlaid on a HST V and I band image. Half of the mid-infrared emission arises from starburst activity that is completely obscured in the optical, including the brightest mid-infrared knot (knot A). The CVF spectrum of this knot is shown in the lower part of the image displaying strong signatures of massive star formation - the NeIII line and a strong rising continuum above $10\mu\text{m}$.

mergers appear to be the triggering mechanism for the ultraluminous phase. Dynamical shocks and tidal forces are the only mechanisms that can cause transference and compression of sufficient quantities of matter to fuel luminosities in excess of $10^{11} L_{\odot}$.

ISOCAM's spatial scale was sufficient to map the morphologies of local interacting active systems (see Mirabel and Laurent, 1999 for a review) and agree with results from ground-based high resolution images that (optically-faint or invisible) compact sources located in deeply obscured nuclear regions or interaction interfaces dominate the mid-infrared emission (e.g. Soifer et al., 2000; Soifer et al., 2001; Charmandaris et al., 2002; Gallais et al., 2004; Siebenmorgen et al., 2004b). For some sources, diffuse emission between these 'hot-spots' can also contribute significantly to the total mid-infrared emission (e.g. Le Floch et al., 2002; Gallais et al., 2004). This diffuse emission can be enhanced in merging systems that are common among active galaxies.

By probing through the famous characteristic dust lane of the AGN-hosting elliptical galaxy Centaurus A (NGC 5128), imaging with *ISOCAM* revealed a barred 'mini-spiral' located in its central 5 kpc. The mini-spiral was proposed to be tidal debris from a gas rich object that was accreted in the last gigayear (Mirabel et al., 1999; Block and Sauvage, 2000). Evidence of accreted companions in Cen A exists from previous studies of its stellar and gas kinematics (Charmandaris et al., 2000, and references therein). *ISOPHOT* contributed to the accretion scenario through the detection of the northern cold dust shell that is possibly the ISM remnant of a captured disk galaxy (Stickel et al., 2004). As a result Cen A is a prime example of a giant elliptical that must have experienced several minor mergers. It is likely that, as the interactions took place, tidal forces funnelled gas into the dynamical centre and boosted the star formation rates in the gas rich components forming the dust observed in the infrared and visible.

4.1.1. Nuclear and extra-nuclear starbursts

Disturbed morphological signatures such as rings, tidal tails, bridges and arcs are clearly detected in *ISOCAM* observations of numerous merging galaxies (e.g. the Antennae (Mirabel et al., 1998) Fig. 2; UGC12915,12914 (Jarrett et al., 1999); NGC 985 (Appleton et al., 2002); Arp 299 (Gallais et al., 2004)). The mid-infrared morphologies depend upon the mass ratio of the progenitor galaxies and the merger stage. As well as enhancing star formation in the nuclear regions, interactions cause a general increase in the widespread activity of the parent galaxies. At the early stages of interaction, wide scale star formation can be induced and dust grains are heated by a generally warmer radiation field. For example, *ISOCAM* observations of the VV 114 galaxy show that 60% of the

mid-infrared flux arises from a diffuse component that is several kpc in size (Le Floc’h et al., 2002). Nearly forty percent of the 7 and $15\mu\text{m}$ emission detected in the early-stage merger (nuclei separation 5kpc) galaxy pair Arp 299 (NGC 3690 and IC 694) is diffuse and originates from the interacting disks (Gallais et al., 2004). In more advanced mergers, shocks and gravitational instabilities encourage the onset of star formation. The transfer of matter to nuclear regions and compression in interaction zones gives rise to enhanced mid-infrared emission in nuclear and often extra-nuclear sites. A clear example of extra-nuclear star formation was uncovered by *ISOCAM* in the intra-group medium of Stephan’s Quintet (Xu et al., 1999).

The best example of *ISOCAM*’s capability in probing through highly extinguished regions is imaging of the spectacular major merger in the Antennae (Arp 244, NGC 4038/4039). The completely obscured overlap region in the HST-WFPC2 image ($A_V \sim 35\text{mag}$ Verma et al., 2003) was shown by *ISOCAM* to contain a massive star forming region ($\lesssim 50\text{pc}$ in radius) comprising more than 15% of the total 12- $17\mu\text{m}$ luminosity which outshines the two nuclei by a factor of 5 (Mirabel et al., 1998). The warm mid-infrared emission traces the molecular gas that fuels star formation (Wilson et al., 2000; Wilson et al., 2003) whereas the cold ($T \sim 30\text{K}$) and very cold dust ($T \sim 20\text{K}$) are traced by far-infrared *ISOPHOT* and sub-mm observations (Haas et al., 2000a). Haas et al. (2000a) find that the sub-millimetre knots, in particular K2, are likely to be in a pre-starburst phase and the simultaneous presence of powerful off-nuclear starbursts & pre-starbursts may be a general feature of colliding galaxies. The authors postulate that once star formation has commenced in these clouds, the Antennae may evolve from a luminous IR galaxy into an ultraluminous one.

An interesting feature for the Antennae (also seen for Centaurus A) is that the most luminous $15\mu\text{m}$ knots are not coincident with the darkest, most prominent dust absorption lanes seen in the HST image. Presumably the darkest optical dust lanes trace the coldest emission (i.e. that probed by the far-infrared) rather than the warm dust from which $15\mu\text{m}$ emission arises. This is plausibly the cause of the displacement. Alternatively projection effects may be responsible for this offset (Mirabel et al., 1998).

Extranuclear overlap starbursts emitting in the mid-infrared are not unique to the Antennae. In a sample of 8 spiral-spiral pairs with overlapping disks, Xu et al. (2000) found extranuclear, overlap region starbursts in 5 galaxies classified as advanced mergers or having severely disturbed morphologies (but not in less disturbed systems). However, the starbursts in the bridges or tidal tails are generally fainter than those in the nuclear regions.

4.1.2. Collisional Rings

Collisional ring galaxies are produced when a compact galaxy passes through the centre of a larger disk galaxy giving rise to a radial density wave that creates a massive star forming ring (see review by Appleton and Struck-Marcell, 1996). If the collision is off centre then the ring morphology is asymmetric e.g. as in VII Zw 466 (Appleton et al., 1999). These systems are excellent local examples of induced star formation in colliding galaxies. The effects of collisions on the ISM can be investigated in detail, and may be relevant for higher redshift galaxies including ULIGs (Appleton et al., 2000). Azimuthal variations in overdensity in the rings are often noted as well as extranuclear star forming knots that show strong UIBs (Charmandaris et al., 1999; Appleton et al., 1999; Charmandaris et al., 2001b; Appleton et al., 2002). When detected, star formation in the ring contributes at a level of $\gtrsim 10\%$ of the bolometric output (Appleton et al., 1999; Appleton et al., 2000). The mid-infrared emission is clearly enhanced in the nucleus and the expanding ring even though diffuse emission from the intervening medium was also observed (Charmandaris et al., 1999; Charmandaris et al., 2001b). The diffuse components coincide with regions where only weak $H\alpha$ had been previously measured. The mid-infrared colours measured in collisional ring galaxies are similar to those of late-type galaxies, indicative of more modest star formation than is found for extranuclear starbursts (e.g. in the nucleus inner ring and spokes of Cartwheel, the entirety of Arp10 and the ring of Arp 118 (Charmandaris et al., 2001b)). The morphological agreement between the mid-infrared and $H\alpha$ or radio emission is good although differences have been noted for VII Zw 466 (Appleton et al., 1999). A deviation from this picture is seen for the extranuclear starburst knot in the archetypal collisional ring galaxy, the Cartwheel, that coincides with the strongest $H\alpha$ and radio knot. The region has an unusually red mid-infrared colour ($15/7\mu\text{m} \sim 5.2$) which is the highest among the extragalactic regions observed with *ISOCAM* and it is even more extreme than the powerful starburst region (Knot A) revealed in the Antennae (Charmandaris et al., 1999). Interestingly this region also hosts the remarkable hyperluminous X-ray source ($L_{0.5-10\text{keV}} \gtrsim 10^{41}$ ergs/s Gao et al., 2003) which dominates the X-ray emission from the Cartwheel ring.

4.2. HOT STAR POPULATION, STARBURST EVOLUTION & METALLICITY

Starburst galaxies, defined as having star formation rates that cannot be sustained over a Hubble time, are likely the birthplace of a large fraction of massive stars. Locally, four starburst galaxies can account

for 25% of the local massive star population within 10Mpc (Heckman et al., 1998) and are important as the providers of the Lyman continuum photons that ionise hydrogen. *ISO* spectroscopy enabled the stellar populations of starbursts to be probed using fine structure lines that are sensitive to the nebular conditions from which they originate (see Förster Schreiber et al. (2001) for a detailed analysis of the stellar populations and radiation environment of the local starburst M 82). The ratio of $[\text{NeIII}]15.6\mu\text{m}$ ($E_p=41\text{eV}$) and $[\text{NeII}]12.8\mu\text{m}$ ($E_p=22\text{eV}$) is sensitive to the hardness of the stellar energy distributions of the OB stars which excite them. In a survey of 27 starburst galaxies, Thornley et al. (2000) confirmed earlier ground-based results that the excitation measured by the $[\text{NeIII}]15.6\mu\text{m}/[\text{NeII}]12.8\mu\text{m}$ ratio was lower in starburst galaxies than measured for Galactic H II regions, indicating a deficiency of massive stars in the starbursts. Thornley et al. suggest a lower upper mass cut-off to the initial mass function (IMF) or ageing of the massive star population to be responsible for the low excitation. Through extensive quantitative photo-ionisation modelling, Thornley et al. found the ratios to be consistent with the *formation* of massive stars (50-100 M_\odot). This, together with the known presence of very massive stars in local starburst regions, led Thornley et al. to prefer an ageing scenario to explain the low excitation. This explanation was further supported by modelling presented in Giveon et al. (2002). The modelling of Thornley et al. indicates a short starburst timescale of only a few O star lifetimes (10^6 - 10^7 yr) and suggests that strong negative feedback regulates the star-forming activity. Disruption due to stellar winds and SNe may cease the starbursts before the depletion of gas and suggests that periodic starburst events are likely (e.g. in M82 Förster Schreiber et al. (2001)).

Verma et al. (2003) confirmed that for a given nebular abundance, local starburst nuclei are of lower excitation than Galactic and Magellanic cloud H II regions. This was shown for the primary products of nucleosynthesis argon, sulphur and neon confirming the Thornley et al. (2000) result was not restricted to Ne only. Additionally, the observed excitation was confirmed to be metallicity dependent, with the lowest metallicity compact dwarfs showing the highest excitations, at a similar level to local H II regions. Ageing, a modified IMF and metallicity are all possible contributors to the metallicity-excitation relation. In the same study the abundance of sulphur was observed to be lower than expected for a primary product of nucleosynthesis. Wolf-Rayet and BCD galaxies did not show such an under-abundance (Verma et al., 2003; Nollenberg et al., 2002). This underabundance and weakness in the sulphur line strength implies that (a) the fine structure lines of neon are favoured over the those of sulphur as a star formation

tracer in future spectroscopic surveys of galaxies and (b) that sulphur is an unsuitable tracer of metallicity.

4.3. WOLF-RAYET STARBURSTS

The Wolf-Rayet phase is a signature of massive star formation as the progenitors are believed to be massive young O stars ($3 \lesssim t_{sb} \lesssim 8 Myr$, $M \gtrsim 20 M_{\odot}$). Wolf-Rayet features are found in a wide range of galaxies such as BCD's, HII galaxies, AGN, LINERs and starbursts (see Schaerer et al., 1999 for a compilation). Recently, Lípari et al. (2003) identified possible Wolf-Rayet features in the spectra of some PG quasars. The identifying Wolf-Rayet signatures are in the visible and thus are only representative of the unobscured components. Nevertheless a correlation between the star formation indicator $U\text{IB}7.7\mu\text{m}/15\mu\text{m}$ continuum with $H\alpha$ in Wolf-Rayet galaxies suggests that the infrared and visible trace, at least partly, the same components (e.g. in Haro 3 Metcalfe et al., 1996). The short-lived Wolf-Rayet phase is commonly detected in low metallicity systems with a strong ISRF such as blue compact dwarfs (BCDs, see Sec. 4.4). *ISO* observations of known Wolf-Rayet galaxies reveal differences in their infrared properties compared to non-Wolf-Rayet galaxies. In comparison to starbursts, Wolf-Rayet galaxies are of higher excitation and lower abundance contrary to expectation of a more important role of Wolf-Rayet stars at higher metallicities from stellar evolution models (Verma et al., 2003). The Wolf-Rayet galaxy NGC 5253 has a weaker excitation determined from mid-infrared *ISO* data than expected by stellar models (Crowther et al., 1999) implying that the UV spectrum may not be as hard as commonly thought. However, Crowther et al. (1999) show that the effect is due to a young compact starburst surrounded by an older starburst both of which lie within the SWS aperture. As a result, measured line strengths are diluted and the apparent effective temperature of the emitting region is lowered thus reducing the measured excitation. This effect, that is fully consistent with an ageing/decaying starburst scenario suggested by Thornley et al. (2000), can explain the low excitation of starbursts described in Section 4.2 (Thornley et al., 2000; Verma et al., 2003).

4.4. BLUE COMPACT DWARFS

A number of low metallicity ($Z \ll Z_{\odot}$) blue compact ($< 5 \text{kpc}$) dwarf galaxies were also observed by *ISO*. These include I Zw 36 (Mochizuki and Onaka, 2001; Nollenberg et al., 2002); Haro 11 (Bergvall et al., 2000), Haro 3 (Metcalfe et al., 1996), NGC 5253 (Crowther et al., 1999), II Zw 40 (Schaerer and Stasińska, 1999; Madden, 2000), NGC 1569

(Madden, 2000; Haas et al., 2002; Lu et al., 2003; Galliano et al., 2003), NGC 1140 (Madden, 2000)). Super-star clusters (SSCs) have been identified within some of them which are likely to be sites of massive star production that generate the bulk of the ionising flux (Gorjian et al., 2001; Vacca et al., 2002; Vanzi and Sauvage, 2004)). These clusters can also account for a substantial fraction of the emerging mid-infrared emission (e.g. Vacca et al. (2002)). The high obscuration, hot infrared emission and thermal radio spectra (measured for some) imply these are embedded young clusters. The properties of BCDs are similar to low metallicity regions in the SMC (Contursi et al., 2000). Some BCDs also exhibit Wolf-Rayet features in their nuclear regions indicative of young massive stars producing a significant amount of ionising UV photons (see Section 4.3). *ISO* observations (see Madden, 2000 for a review) reveal varying characteristics between BCDs although fine structure lines common to starbursts are present e.g. [OIV], [SIII,IV] and [NeII,III] with ratios that indicate high excitation (e.g. Crowther et al., 1999). The low metallicity and dust mass of BCDs in comparison to normal galaxies permits photoionisation on galaxy wide scales (Madden, 2000). UIBs are weak or absent due to destruction of their carriers by the intense radiation field and the mid-infrared is dominated by a strong VSG continuum. [CII]/(CO) emission (and [CII]/FIR to a lesser degree) can be greatly enhanced ($\times 10$) in comparison to normal metallicity starburst galaxies (Bergvall et al., 2000; Madden, 2000). Along with the hot dust detected in BCDs (e.g. Metcalfe et al., 1996), very cold dust components were surprisingly observed in some BCD members of the Virgo cluster (Popescu et al., 2002) and in NGC 1569 (Galliano et al., 2003). In the latter, a very cold component ($T=5-7\text{K}$) contributes between 40-70% of the total dust mass of the galaxy. Molecular gas (CO) and infrared emission indicate that, although relatively metal poor, these dwarfs have high dust and gas densities for their optical sizes (Mochizuki and Onaka, 2001).

An exceptional BCD is SBS 0335-052, one of the most metal poor galaxies currently known ($1/41Z_{\odot}$). This dwarf harbours obscured, central SSCs (Dale et al., 2001b; Hunt et al., 2001) and shows a young thermal radio spectrum (Takeuchi et al., 2003; Hirashita and Hunt, 2004). SBS 0335-252 is unusually bright in the mid-infrared. No UIBs have been detected and the [SIV] and [NeII] lines are weak in comparison to the strong continuum (Thuan et al., 1999). Estimates of the optical depth vary between authors from optically thin (Dale et al., 2001b) to $A_V \sim 10-30$ (Thuan et al., 1999; Plante and Sauvage, 2002). The current optical, radio and infrared measurements make it difficult to present a consistent scenario for this intriguing galaxy. Further observations are needed to elucidate how such a small galaxy can produce

such strong infrared emission without polluting its ISM with metals (Thuan et al., 1999).

4.5. STAR FORMATION RATES

The non-linear correlation (with large dispersion) between the far-infrared and $H\alpha$ emission in normal galaxies (Sauvage and Thuan, 1992) suggests the use of the far-infrared as a direct SFR estimator has limitations (Kennicutt, 1998). At least for normal galaxies, both a contribution from the nuclear regions (Roussel et al., 2001) as well as from cold dust that is unrelated to the starburst activity may be responsible for the non-linear behaviour. At the highest infrared luminosities, such as in a sample of ULIGs, this very cold component comprises only $\lesssim 10\%$ of the total far-infrared flux (Klaas et al., 2001). However, for less luminous sources that often have more dominant very cold components (e.g the starbursts in Calzetti et al., 2000), the contribution to the far-infrared from heating from non-ionising, older stars should be considered when SFRs are determined (Lonsdale Persson and Helou, 1987). A more basic problem is that SFR estimates based on the far-infrared flux are prone to errors arising simply from poorly determined far-infrared luminosities due to inadequate sampling or constraints on the far-infrared SEDs. This affects often the faintest most luminous sources detected in *IRAS* and *ISO* flux limited surveys where for some sources only one or two far-infrared data points are available.

The mid-infrared also provides an alternative measure of the SFR. Based on *ISO* data for a large sample of non-AGN-hosting galaxies, Dale et al. (2001a) highlighted that, rather than the commonly used far-infrared flux ($42\text{-}122\mu\text{m}$), the mid-infrared SED between $20\text{-}42\mu\text{m}$ is most sensitive to the level of star formation activity. Additionally, the correlation of the mid-infrared flux $7\mu\text{m}/15\mu\text{m}$ flux ratio with optical tracers of star formation such as $H\alpha$ in a range of galaxies (e.g. in normal galaxies (Sauvage et al., 1996; Roussel et al., 2001), Wolf-Rayet galaxies (Metcalf et al., 1996), mixed pair local interacting galaxies (Domingue et al., 2003; Domingue et al., 2005), collisional ring galaxies (Charmandaris et al., 2001b), other interacting galaxies (Le Floch et al., 2002)) and the mid-infrared H-recombination lines, that are correlated to the Lyman continuum, shows that the mid-infrared flux can be used as a SFR indicator (Vigroux et al., 2001; Förster Schreiber et al., 2004). Förster Schreiber et al. (2004) provide an empirical calibration of the UIB flux between $5\text{-}8.5\mu\text{m}$ range as a SFR estimator which is valid for starbursts up to the rate of M82, close to which the ISRF causes sublimation of the UIB carriers. The VSG continuum represented by the monochromatic $15\mu\text{m}$ flux, that has been shown

to correlate well with the [ArII]6.99 μ m line (Förster Schreiber et al., 2003), can withstand harder radiation fields providing a SFR estimator for higher redshift, more luminous sources. A potential scatter in this correlation can be introduced by an AGN contribution to the VSG continuum; an event that may become more common in galaxies of high luminosity (Sect. 6.5). In this case the mid-infrared may not be a direct indicator of the SFR unless the AGN contribution can be accurately subtracted (Laurent et al., 2000).

4.6. FIR SPECTROSCOPY & THE [CII] DEFICIT

The far-infrared spectrum of the starburst galaxy M 82 (Colbert et al., 1999) shows several fine structure lines including those that are commonly detected in active galaxies: [OI]63,145 μ m; [OIII]52,88 μ m; [NII]122 μ m; [NIII]57 μ m and [CII]158 μ m. These features are superimposed on a strong thermal continuum. [CII]158 μ m, along with [OI]63,145 μ m and [NII]122 μ m, are important cooling lines of star forming regions and have been shown to correlate with the dust continuum over 4 orders of magnitude in the Galaxy (Baluteau et al., 2003). For many galaxies, especially those with low metallicities, [CII]158 μ m is the strongest far-infrared line, corresponding to 0.1-1% of the far-infrared flux (Malhotra et al., 1997; Madden, 2000; Bergvall et al., 2000). The spatial correlation of the [CII]158 μ m emission with obscured regions and the fact that it scales linearly with UIB and CO relative strength suggests it originates in PDRs (Unger et al., 2000; Malhotra et al., 1997; Malhotra et al., 2001; Masegosa et al., 2001). Fitting of the LWS spectrum of M82 confirms this view with 75% of the line produced in PDRs and the remainder from H II regions (Colbert et al., 1999) while, for a sample of nearby galaxies, Negishi et al. (2001) find half to originate in PDRs and half in low density ionised gas.

The spectra of active galaxies range from those exhibiting strong ionic fine structure emission lines (such as M82) to molecular absorption line dominated systems (such as Arp 220) (Fischer et al., 1999b; Fischer, 2000). The fine structure lines that are predominant in starburst galaxies are absent or weak in the spectra of higher luminosity (Malhotra et al., 1997; Fischer et al., 1997; Fischer et al., 1999b; Fischer et al., 1999a). In particular, the [CII]158 μ m/FIR continuum ratio decreases with increasing luminosity (Malhotra et al., 1997) and in ULIGs is only 10% of that measured for starbursts (Luhman et al., 1998; Fischer, 2000; Luhman et al., 2003) and is even lower in LINERs (Sanei and Satyapal, 2002). As an important cooling line of warm atomic gas, [CII] was expected to be high for strongly star-forming galaxies with a high UV radiation field. Contrary to intuition, the absence of the fine

structure lines and the strong molecular absorption detected (e.g. OH, H₂O, CH, NH₃ and [OI]) imply a weaker radiation field in ULIGs in comparison to nearby starbursts and AGN that is probably caused by shielding (Fischer, 2000).

For sources deficient in [CII]158, the [OI]63,145 μ m lines appear to become the preferred means of cooling star forming gas (Malhotra et al., 1999; Brauher and Lord, 2000). In a systematic survey of LWS spectra of 36 local galaxies, Negishi et al. (2001) found a strong decrease in the the [CII]158 μ m/FIR and [NII]122 μ m/FIR cooling line ratios with bluer far-infrared colours. However no such trend was seen for [OI]63/FIR implying that the oxygen lines do not suffer from the [CII] deficiency.

A number of explanations have been proposed for the [CII] deficit. Tracing [CII] towards the Sgr B2 complex, which has an intense radiation field and gas density similar to active galaxies, raises the possibility that self-absorption may contribute to the observed deficiency (Cox et al., 1999). The [CII]158 μ m line is seen both in emission (originating from Sgr B2) and absorption (Vastel et al., 2002) consistent with the presence of intervening (cold) clouds along the line of sight. This indicates the [CII]158 μ m can be optically thick. However, the weakness of the [OI]145 μ m line observed in Arp 220 and Mrk 231 and the large extinctions implied ($A_V \gtrsim 400$, that exceed most other extinction measurements but see Haas et al. (2001) for Arp 220) pose problems for solely a self-absorption explanation of the [CII]/FIR deficiency (Luhman et al., 2003). Lower efficiency of photoelectric gas heating for high radiation fields, such as those in the PDRs of active galaxies, has been suggested (Malhotra et al., 1997) but an accurate analysis of this scenario remains to be performed. Additionally, the radiation field and gas density may play a role. Ageing bursts were discounted because of the detection of the high excitation lines [NeIII] and [SIII] and because older starbursts are unlikely to fuel such high luminosities (Fischer et al., 1999a). Increased collisional de-excitation, rather than the decrease in the photoelectric heating efficiency, was supported by Negishi et al. (2001). Luhman et al. (1998) proposed high UV flux incident on moderate density PDRs to explain the deficiency. However, in a revision of this work, (Luhman et al., 2003) preferred a non-PDR contribution to the far-infrared to explain the deficiency in the [CII]/FIR ratio. The authors suggest dust-bounded photoionisation regions as a possible origin since such regions contribute to the far-infrared (i.e. increased UV-absorption by dust) but do not generate significant amounts of [CII]. This interpretation is corroborated by the increasing fraction of dust-absorbed photons with ionisation parameter (Voit, 1992). This scenario is also preferred in the radiative-transfer

models of Arp 220, although the effects of extinction cannot be ruled out (González-Alfonso et al., 2004) .

The [CII] deficiency affects possible future searches of [CII]158 μ m line emission from high redshift sources that have similar rest-frame far-infrared colours to local ULIGs. Moreover, if the stronger cooling line in warmer infrared galaxies is [OI]63 μ m, then the recent non-detections in four $z=0.6-1.4$ ULIG-quasars (Dale et al., 2004) also indicate a pessimistic view on either of these lines as high-redshift tracers of active galaxies. The [OI]63 μ m line may also be self-absorbed.

4.7. GAS-TO-DUST RATIO AND STARBURST EVOLUTION

The gas-to-dust ratio is commonly used as an indicator of the fraction of gas that is yet to be turned into stars. Dust mass estimates determined from *ISO* SED analyses are used for this determination. The gas-to-dust ratios determined for starbursts, ULIGs, and quasars, are similar or only slightly larger ($\sim 150-400$) than those determined for the Milky Way (~ 150) (Calzetti et al., 2000; Haas et al., 2003). The highest gas-to-dust ratios are seen in BCD galaxies indicating young stellar evolution (Dale et al., 2001b). Low gas-to-dust ratios and low dust temperatures indicate a post-starburst system (e.g. the radio galaxy MG1019+0535 (Manning and Spinrad, 2001) and HyLIG F15307+3253 (Verma et al., 2002)).

5. Warm dust and hard radiation fields: nuclear AGN

5.1. AGN IN MERGERS

ISO's low spatial scale could not discern emission from the torus and circumnuclear starburst regions even in the most nearby active galaxies. As AGN emission is unresolved in *ISOCAM* images, in this section we discuss the environment of the AGN, i.e. the heating of the ISM of the host galaxy. The collisional ring galaxies NGC 985 and Arp 118 both host Seyfert nuclei. In NGC 985, near-infrared images resolve the bulge of a small, second galaxy (whose accretion likely led to the formation of the ring) near the active bright nucleus (Appleton et al., 2002). The nuclei in both of these galaxies show a hot mid-infrared continuum that can wholly be attributed to dust heating by active nuclei. UIB emission is suppressed around the nuclei, suggesting they are absent in the vicinity of the AGN. In the case of Arp 118, the Seyfert nucleus accounts for 75% of the mid-infrared emission from the galaxy. Two other LIGs, VV 114 and Arp 299, show strong and hot mid-infrared continuum emission, i.e. that hot dust is present (a 230-300K blackbody

describes the VSG hot continuum), indicating that embedded AGN may reside within these galaxies (Le Floc'h et al., 2002; Gallais et al., 2004). Seyfert nuclei seem to have high mid-infrared luminosities, as well as contributing significantly to the total mid-infrared emission of the system. In three merging pairs of ULIGs within which one member contains an AGN, the AGN hosting galaxy is invariably more infrared luminous than the other (Charmandaris et al., 2002). Mirabel and Laurent (1999) note that the most luminous sources are those that exhibit both AGN and starburst activity, reflecting the well known trend of increasing AGN importance with infrared luminosity (see Sec. 6).

5.2. WARM SEDS

ISO observations of the $12\mu\text{m}$ *IRAS* galaxy sample (Rush et al., 1993), that consists predominantly of Seyfert 1 and 2s but includes starbursts and normal galaxies, displays a range of SED shapes that can be expected for these source types (see Figure 2 in Spinoglio et al. (2002)). These average SEDs show clear differences between normal galaxies, starbursts and the Seyferts in the optical to mid-infrared range, but they appear indistinguishable in the far-infrared.

By approximating the Seyfert SEDs using black-body functions, authors such as Rodriguez Espinosa et al. (1996) or Antón et al. (2002) found that two components best fit their SEDs where the warmer component was associated to the active nucleus and the colder component with star forming or extended regions. Similar associations were made for the two (or three) components implied by a novel inverse Bayesian method to analyse the SEDs of 10 Seyfert galaxies (Perez Garcia et al., 1998). Prieto et al. (2001) showed that the fluxes of high excitation coronal lines detected in the *ISOSWS* spectra of Seyfert galaxies, which are ascribed to excitation by the intense radiation field of the active nucleus, were found to be correlated to this mid-infrared component but not to the far-infrared component. This implies that the mid-infrared component arises from dust heated by processes related to the active nucleus.

5.3. IONISATION IN AGN AND SEYFERTS: THE BIG BLUE BUMP

A thin accretion disk that fuels a black hole displays a generic signature (quasi-thermal photons at $T \sim 10^5$) in the extreme UV (EUV) commonly called the big blue bump (BBB). The bump is likely to extend from the UV towards the soft X-ray bump but, due to galactic and intrinsic absorption between the Lyman edge and a few hundred eV, the peak of the bump is not directly detectable. A novel method to reconstruct the BBB is to use the high ionisation potential infrared fine structure lines

(coronal lines, 50-300eV) that originate in the narrow-line region of Seyferts and quasars and directly probe the EUV SED. Reconstruction of the BBB was attempted using photo-ionisation modelling of the Seyferts NGC 4151 (Sey 1.5), NGC 1068 (Sey 2) and Circinus (Sey 2). The reconstruction is not only dependent upon the ionising continuum but also on the geometry of the NLR and the ionisation parameter. It was possible to constrain the presence of this bump for these galaxies by complementing the ISO data with UV, optical, and near-infrared lines. All three investigated sources (Moorwood et al., 1996; Alexander et al., 1999c; Alexander et al., 2000) require the presence of a thermal blue bump, a single power law continuum fails to reproduce the observed narrow line ratios. Circinus provides the clearest example of an EUV bump that peaks at 70eV and contains half of the AGN luminosity. The predicted SEDs of NGC 4151 and NGC 1068 display clear troughs falling sharply beyond the Lyman limit and rising sharply above 100eV. The preferred explanation is that it is due to absorption by neutral hydrogen of column density $N_H \sim 5 \times 10^{19} \text{cm}^{-2}$. In the case of NGC 4151 this absorbing gas was identified through an analysis of UV absorption lines (Kriss et al., 1995). This scenario allows for the presence of (obscured) BBB in all of the sources investigated (see also Prieto et al. (2001)). However, Binette et al. (1997) find that photoionization by a simple power law suffices to explain Circinus, if an optically thin (density-bounded) gas component is included. In a detailed metallicity analysis, Oliva et al. (1999) find that either approach can equally explain the observations, and note that the ionising continuum is mostly dependent upon the gas density distribution. More complex geometry and distribution of gas (e.g. 3-D multi-cloud models) and emission mechanisms (shock heating and photoionisation) (Contini et al., 1998; Contini et al., 2002; Martins et al., 2003), than an assumed single cloud with filling factor < 1 (Alexander et al., 1999c), are more appropriate assumptions to model the narrow-line emission properties surrounding AGN (Martins et al., 2003).

While such detailed modelling was not possible for less well observed sources, a comparison of spectroscopic tracers, such as electron density and excitation, to photoionisation models enabled at least a consistency check to be performed between power-law or black-body continua. However, neither Sturm et al. (2002) nor Prieto et al. (2001) were able to distinguish the two for their sources with the range of lines they used. The metallicity, geometry and density of obscuring clouds and extinction all play a role in these analyses.

5.4. THE DUSTY TORUS AND VARIABILITY

If near and mid-infrared emission from the inner region of AGN is thermal re-radiation by dust surrounding the central engine then, over sufficiently long timescales, variability seen in the optical/UV should be detectable in the infrared. This would provide convincing proof and constraints on the presence, temperature and distribution of dust grains from the variable source. However *ISO* monitoring of variable AGN, that were contemporaneous to other multiwavelength campaigns, failed to show any convincing thermal variability (e.g. Mrk 279 Santos-Lleó et al., 2001; BL Lac PKS 2155-304 Bertone et al., 2000; BL Lac 2007+777 Peng et al., 2000; OVV quasar 3C 446 Leech et al., 2002). Rather, the variability where detected, was consistent with non-thermal components such as jets (Peng et al., 2000; Leech et al., 2002).

These findings are consistent with variability traced by polarisation measurements of the OVV quasar 3C 279 at $170\mu\text{m}$ (Klaas et al., 1999) showing that the polarisation detected was aligned to the radio axis and thus consistent with synchrotron emission. The rapid variability noted in two measurements separated by $\sim 1\text{yr}$ confirms that the far-infrared emission is compact and originates from the core.

5.5. UNIFICATION

Under the standard unification scheme (Antonucci, 1993), the orientation relative to the line of sight of a dusty putative torus surrounding the accretion disk of the central black hole, may connect various types of active galaxies: radio galaxies to quasars and Seyfert 1s to Seyfert 2s. A check of these schemes is offered through their infrared emission: the dust torus intercepts optical-UV photons released by the AGN and re-emits them in the infrared. At $\lambda > 30\mu\text{m}$ the infrared emission is largely optically thin and hence isotropic. As a result the infrared SEDs should be similar for all members of a unified class, irrespective of the orientation of the obscuring torus to the line of sight. In this section we discuss how *ISO* results have contributed to understanding this issue.

5.5.1. *Radio galaxies and quasars*

Orr and Browne (1982) and Barthel (1989) proposed a scheme that unifies quasars and radio galaxies as intrinsically similar sources, with observed differences ascribed to the viewing-angle with respect to the black hole. A quasar with a flat radio spectrum is observed with a viewing- or aspect-angle of 0° to the line of sight (pole-on) such that a beamed jet with superluminal motion causes the bright radio and far-infrared appearance (e.g. FR 0234+28). At intermediate angles between the pole- and edge-on orientations, a quasar with a steep radio spectrum

is seen. The shallower the aspect angle, the more obvious the thermal bump of the torus becomes. At large orientations (90° or perpendicular) to the line-of-sight, we observe the radio galaxy with the torus edge-on (e.g. Cyg A, Fornax A, Centaurus A) whereby the nucleus that contains an “optical quasar” is obscured by the dusty torus. Powerful Fanaroff-Riley (FR) II radio galaxies are “edge-on” quasars viewed at high inclination (Haas et al., 1998a). Overwhelmingly for samples of radio galaxies and radio quasars their SEDs appear indistinguishable in the far-infrared (Haas et al., 1998a; van Bemmel et al., 2000; Meisenheimer et al., 2001; Andreani et al., 2002; Haas et al., 2004) confirming the expectation from unified schemes i.e. that the dust is isotropic and optically thin. This is contrary to indications from *IRAS* data that implied radio galaxies have lower mid-far infrared emission than radio quasars. The lower redshift range probed by *IRAS* may account for this (Meisenheimer et al., 2001).

5.5.2. *Narrow line radio galaxies; broad line radio galaxies and quasars*

The 3C sample of quasars selected at 178MHz contains two types of galaxies: (1) those exhibiting broad lines: steep spectrum quasars and broad line radio galaxies; and (2) those exhibiting narrow lines: FR II narrow line radio galaxies. Under the unification scenario, sources of identical isotropic lobe power should have the same far-infrared isotropic power. Haas et al. (2004) confirm earlier results of Meisenheimer et al. (2001) for *all* 3CR sources present within the *ISO* Data Archive¹, providing clear evidence in favour of geometric unification. The considerable dispersion in lobe power can be attributed to environment and evolution. Siebenmorgen et al. (2004a) confirm earlier work of Freudling et al. (2003) and find that the SEDs of narrow-line radio galaxies to be colder ($\lambda_{peak} \sim 100\mu\text{m}$) than the broad-line counterparts ($\lambda_{peak} \sim 40\mu\text{m}$). This result is fully consistent with unification schemes where, in broad-line radio galaxies, the BLR is exposed and so is hot dust that causes the SED shape to appear warmer.

5.5.3. *FR I and FR II galaxies*

These extended radio sources are separated by the fact that FR II galaxies show powerful edge-brightened extended double lobes whereas FR Is have diffuse lobes that are brightest close to the nucleus. Moreover, FR Is are of lower luminosity than FR IIs. In a recent study of 3CR sources, Müller et al. (2004) found that the low radio power FR I galaxies have low mid- and far-infrared luminosities. In contrast, the FR

¹ <http://www.iso.vilspa.esa.es>

II sources are infrared luminous. The high far-infrared-to-mid-infrared ratio and the temperature of the far-infrared peak which is comparable to that of quiescent radio-quiet elliptical galaxies, implies that heating by the ISRF of the host galaxy is probable. This together with the finding that the dust masses of FR Is and FR IIs are similar but with low gas fractions in the nuclear regions, implies that the black holes in FR I galaxies are fed at a lower rate than FR II galaxies (Müller et al., 2004).

5.5.4. *Flat spectrum and Steep spectrum Quasars*

Flat spectrum quasars show a strong synchrotron component (e.g. FR 0234+28), smoothly concatenating the mm flux to that observed in the mid-infrared (Haas et al., 1998a). A thermal far-infrared component may equal the synchrotron in strength (e.g. 3C 279), but in most cases only upper limits to a thermal contribution can be derived due to the dominating synchrotron emission. This prevalence of far-infrared synchrotron emission is consistent with Doppler boosted synchrotron emission of a relativistic jet seen almost end-on and does not contradict this unification (Haas et al., 1998a).

5.5.5. *Radio-loud and radio-quiet quasars*

A complete range of radio-loud, radio-intermediate and radio-quiet quasars was analysed by Polletta et al. (2000). Except for flat radio sources, the mid- and far-infrared emission is of thermal origin. The far-infrared emission is predominantly explained by heating from the AGN itself and, while starburst components are present, they contribute to the infrared emission at different levels but always less than the AGN ($\lesssim 27\%$).

5.5.6. *Seyfert 1s and Seyfert 2s*

Within the unified scheme, Seyfert 1s and 2s differ only in viewing angle of the torus obscuring the central black hole. In Seyfert 1s the broad line region is exposed whereas in Seyfert 2s it is hidden from view due to obscuration by the torus. The central regions where dust is heated to high temperatures gives rise to a mid-infrared peak in the continuum emission. Aspect-oriented unification is consistent with the result that the mid-infrared dust temperatures of Seyfert 1s are higher than in Seyfert 2s, where the torus is partially optically thick up to the mid-infrared (Pérez García and Rodríguez Espinosa, 1998). Spectroscopic tracers such as high excitation lines and broad lines are indicative of the presence and orientation of the putative torus. In a large sample of Seyferts, Clavel et al. (2000) showed that UIB equivalent widths are larger in Seyfert 2s than in Seyfert 1s. An interpretation of this result

is that UIB features originate from extended regions and hence emit isotropically, while the AGN continuum is absorbed by the torus and must emit anisotropically (Pérez García and Rodríguez Espinosa, 2001) since it is dependent upon the orientation of the torus to the line of sight. This interpretation thus provides direct proof of the unification of the Seyfert classes.

A test of unification schemes is offered via observations in hard X-rays that can penetrate an obscuring (Compton-thin) torus. Thus, in the simplest unification models, if X-ray emission is not beamed, the mid-infrared continuum arising directly from AGN heating of the torus or dust in the narrow line region is determined by the geometric distribution of the obscuring material and the aspect angle. After isolating the mid-infrared continuum due to the active nucleus alone, Lutz et al. (2004a) found no distinction between Sey 1s and 2s with the X-ray/mid-infrared flux ratio, contrary to the predictions of unified schemes. The authors suggest the apparent uniformity is due to the dilution of anisotropic emission by a predominant mid-infrared component on extended scales that emits isotropically.

Another result that is difficult to reconcile with the torus model arises from *ISO* SED analysis of a sample of hard X-ray selected sources comprising both type 1 and 2 Seyfert galaxies. Kuraszekiewicz et al. (2003) showed that while Seyfert 2s are redder in their optical colours than Seyfert 1s, their mid- to far-infrared emission, as traced by the 25 to 60 μ m colour, remains similar. More complex geometries for the obscuring material are required to explain both the difference in optical colours and the similarity in the infrared. Clumpy and extended models are suggested where a disk of only a few hundred parsecs can reproduce the IR SED without invoking a starburst component (see Elitzur et al., 2003 and Sect. 6.6).

5.6. EVOLUTION OF COMPACT STEEP SPECTRUM RADIO GALAXIES

ISO data contributed towards understanding whether the compactness of steep-spectrum radio galaxies was due to age or evolution of environmental conditions that inhibits the growth of the radio lobes. It was expected that dense material causing this inhibition should be accompanied by far-infrared emitting dust. However, Fanti et al. (2000) found no far-infrared excess in compact steep spectrum radio galaxies, in comparison to a control sample of 16 extended radio galaxies, which favours a youthful scenario to explain their compactness.

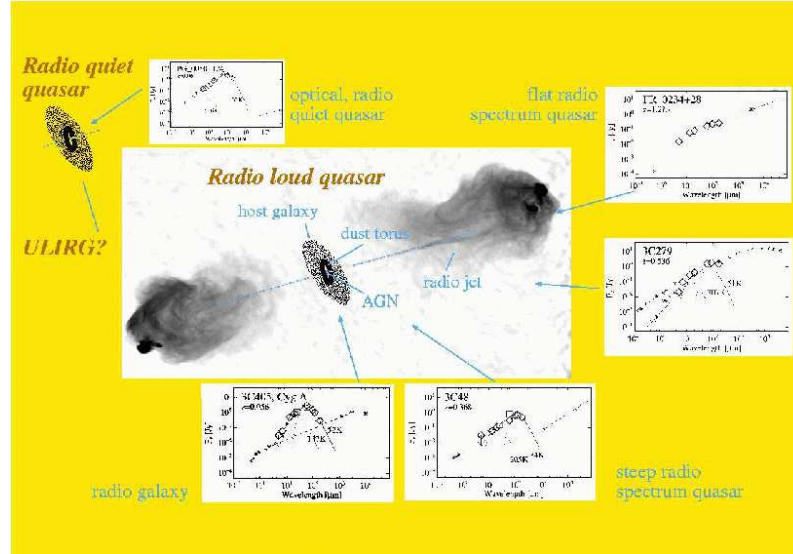


Figure 3. Illustration of the unified scheme of quasars complemented by its manifestation in the infrared SEDs of quasars (Haas et al. 1998).

5.7. CONSTRAINTS FROM LINE PROFILES

5.7.1. Probing the NLR

The emission line profiles of Seyfert galaxies are known to exhibit blue asymmetries and blue-shifts with respect to the systemic velocity in their optical spectra. The profiles provide constraints on the NLR. Narrow lines detected in the mid-infrared have the advantage of being much less sensitive to extinction than optical lines and therefore provide a relatively unobscured view to the NLR. The similarity in line shapes between the optical and the mid-infrared provides constraints on the nature of the NLR and models how such asymmetries were produced. Sturm et al. (1999) are able to rule out simple radial flows plus dust scenarios and they propose that a central geometrically thin, but optically thick, obscuring screen located close to the nucleus is present in NGC 4151 to explain the observed asymmetry. The mid-infrared line profiles of NGC 1068 are due to a combination of an highly ionised outflow and extended emission of lower excitation, and remaining blue shifts attributed to an intrinsic asymmetry in the NLR or very high column density in the line of sight (Lutz et al., 2000b). For a larger sample, Sturm et al. (2002) show that the differences in line profiles depend upon the ionisation potential. Circinus shows symmetric low-ionisation and asymmetric high-ionisation lines while the spectrum of NGC 7582 shows the reverse. These differences suggest that the NLR properties affecting individual galaxies are particular to

that galaxy. Differences including extinction, asymmetric distributions of NLR clouds, orientation must all influence the line shapes (Sturm et al., 2002).

5.7.2. *Probing the BLR*

Lutz et al. (2000a) searched for broad components in the H-recombination lines of NGC 1068, since the detection would imply that at least part of the BLR is accessible in the mid-infrared (looking through the obscuring putative torus). The lack of detection places a lower limit in both extinction ($A_V > 50\text{mag}$) and hydrogen column density ($N_H > 10^{23}\text{cm}^{-2}$). Although little can be stated regarding favoured torus models or constraining gas properties based upon this information, Br α was identified as being the preferred indication for future studies and Lutz et al. (2002) found broad line components in approximately 1/4 of their sample of Seyfert galaxies from ground based high resolution spectroscopy.

6. Ambiguous Sources: Ultra- & hyperluminous infrared galaxies

As we have previously discussed, ULIG samples contain galaxies of both starburst and AGN type. Establishing whether these types are linked in evolution or nature is a key issue in the study of active galaxies raising several questions: what is the role of star formation and black holes; which is/are present; do super-massive black holes and starburst activity concurrently exist in all ULIGs and how much do they contribute to the bolometric luminosity? Prior to *ISO*, few observational tools were available to probe through the dust obscuration to reach the source of the infrared power. *ISO*'s spectroscopic and photometric capabilities enabled significant advances in this field, largely elucidating the previously termed 'starburst-AGN controversy' which is discussed in this section.

6.1. QUANTITATIVE SPECTROSCOPY

6.1.1. *Fine Structure Line Diagnostics*

Fine structure lines directly trace the excitation states of the ISM from which they originate. The radiation fields generated by AGN/QSO greatly exceed that of starbursts and thus can excite interstellar gas to higher ionisation species (as described in Sect. 2.2.2). The difference in excitation between AGN and starbursts is the basis of fine structure line diagnostic diagrams. Such excitation diagrams are well established

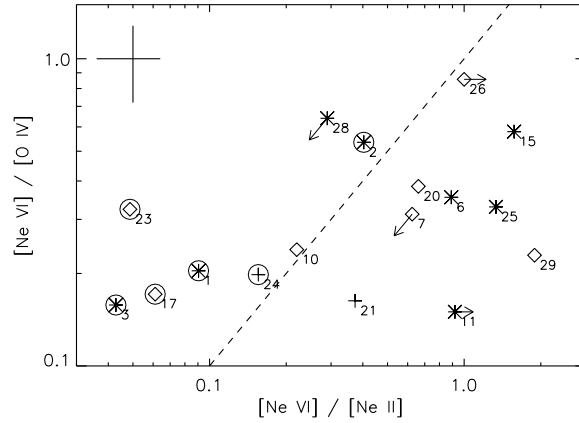


fig. a

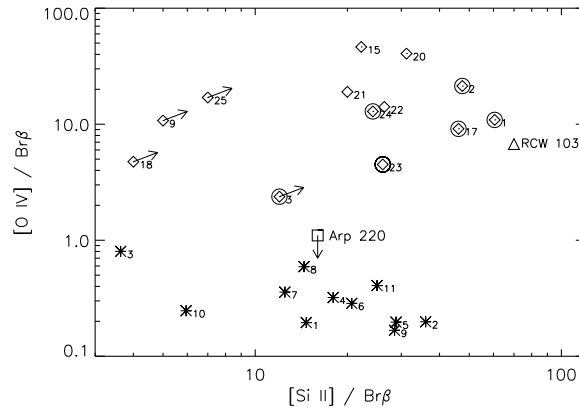


fig. b

Figure 4. Diagnostic diagrams based upon fine structure lines from Sturm et al. (2002). Fig. a: $[\text{Ne VI}]/[\text{O IV}]$ vs $[\text{Ne VI}]/[\text{Ne II}]$: Diamonds - Sey 1s, Asterisks - Sey 2s; the composite Seyfert galaxies that exhibit UIBs are encircled and are mostly separated from the remaining galaxies. Fig. b: $[\text{O IV}]26\mu\text{m}/\text{Br}\beta$ vs $[\text{Si II}]34\mu\text{m}/\text{Br}\beta$: Diamonds - AGN asterisks - Starbursts; the starbursts occupy a different regions of the diagnostic diagram than the AGN.

in the optical (Veilleux and Osterbrock, 1987; Kewley et al., 2001), for which Sturm et al. (2002) constructed the first infrared analogues (Fig. 4) that successfully distinguish starbursts from AGN.

Diagnostic diagrams from Sturm et al. (2002) are shown in Fig. 4 both involving the fine structure line $[\text{O IV}]25.91\mu\text{m}$. While this line was expected in the high ionisation potential of AGN, it was also often weakly detected in star-forming galaxies and ULIGs (Lutz et al., 1998a). In our Galaxy, the $[\text{O IV}]25.91\mu\text{m}$ line has not been observed in H II regions surrounding young, hot, massive stars. However, its detection in *ISO* spectra of starbursts and the fact that it was spatially

resolved in the low excitation starburst M82 implies it is plausibly produced by ionising shocks or extremely hot ionising stars (Lutz et al., 1998a; Schaerer and Stasińska, 1999). Its diagnostic capability thus arises from the fact that the measured strength of the line in starburst galaxy spectra is at least ten times fainter than those measured in spectra of AGN. This absolute difference in the strength of [OIV] relative to a low excitation starburst line such as [NeII] provides a straightforward indicator of AGN versus starburst activity (Sturm et al., 2002).

Combining the high:high excitation fine structure line ratio [NeVI]/[OIV] with the high:low excitation fine structure line ratio [NeVI]/[NeII], provides a basic diagnostic of composite sources (Fig. 4a). By using the limiting values of the high:low excitation ratio [OIV]/[NeII] (always <0.01 in starbursts and $0.1 < \text{AGN} < 1.0$) Sturm et al. (2002) were able to estimate the fractional contribution of an AGN to the bolometric luminosity through a simple mixing model. Fig. 4b shows how the high and low ionisation indicators normalised to the H-recombination line $\text{Br}\beta$ (an indicator of the Lyman continuum rate) provides an analogue to the Veilleux and Osterbrock (1987) diagnostics that are insensitive to obscuration and will be extremely useful for classifying ULIGs observed with future infrared spectrographs. An equivalent diagnostic at longer wavelengths can be constructed using $[\text{CII}]158\mu\text{m}/[\text{OI}]63\mu\text{m}$ versus $[\text{OIII}]88\mu\text{m}/[\text{OI}]63\mu\text{m}$ that can separate starburst, AGN and PDR contributions (Spinoglio et al., 2003).

As the spectroscopic sensitivity of *ISO* permitted the detection of H-recombination lines or useful limits on the [OIV] emission in only the brightest sources, alternative tools using more commonly detected spectral features (e.g. UIBs and bright fine structure lines) were used during earlier *ISO* science analysis. Genzel et al. (1998) combined excitation and UIB strength to assess the nature of a large sample of AGN, starbursts and ULIGs. Laurent et al. (2000) constructed a diagnostic based upon the mid-infrared continuum shape to UIB strength (Sect. 6.1.2). However the use of UIBs is limited and presents problems in interpretation (Sect. 6.1.3).

6.1.2. *UIB-based diagnostics*

The predominance of UIBs in starbursts (and their deficiency in AGN, or low metallicity environments) naturally lends the ratio of UIB feature flux (normalised to the mid-infrared continuum) to be a suitable tracer of star formation activity (Verstraete et al., 1996; Förster Schreiber et al., 2004; Peeters et al., 2004). For normal and starburst galaxies the UIB to continuum ratio is seen to be high in the nuclear star-forming regions and to decrease with radial distance (Mattila et al., 1999; Dale et al., 2000), indicating a weakening ISRF. Conversely, a

strong enhancement in the continuum to line ratio is seen in the vicinity of AGN, where the continuum is strong and UIBs weak as the features suffer dilution due to the absolute high level of the continuum and/or destruction of their carriers (Lutz et al., 1998b). The effectiveness of this indicator is clearly seen in Centaurus A, where spatially resolved *ISOCAM-CVF* observations of the AGN-dominated nucleus and the extended starburst region (Mirabel et al., 1999) show striking differences in their mid-infrared emission. Together with the absence of UIB emission features, the spectral index of the continuum is steeper in AGN than in the surrounding circumnuclear star forming regions. These spectral differences enable, at least in principle, discrimination between the emission characteristics of the two distinct physical mechanisms.

Genzel et al. (1998) demonstrated the effectiveness of the $7.7\mu\text{m}$ UIB-to-continuum ratio versus a tracer of hardness (such as the ratio of the high excitation potential fine structure line [OIV] to the low excitation line [NeII] (or [SIII])) to classify ambiguous sources. This 'Genzel-diagram' (Fig. 5a) enabled the classification of ULIGs for which the underlying fuelling mechanisms were unclear in the pre-ISO era. The separation between AGN, starbursts and the intervening ULIGs is unequivocally depicted. The well known low-excitation starburst M82 is far separated from the AGN NGC 4151. These extremities more or less define an appropriate mixing line that begins with 0% AGN in the lower right corner to 100% in the upper right. Thus placing a ULIG on this plane provides an indication of its AGN fraction. The line of equivalent mixing is marked on the diagram, 4 of the 13 ULIGs shown fall to the left of that line implying a bolometrically dominant AGN is needed to explain their emission.

Similarly, using the ratios of $6.2\mu\text{m}$ UIB-to-continuum vs. warm-to-hot continuum, Laurent et al. (2000) constructed a diagnostic diagram that can quantitatively estimate the fractional contribution from AGN, H II regions and PDRs. Laurent et al. (2000) showed how a mid-infrared spectrum may be quantitatively decomposed into these three components through spectral template fitting (see Fig. 5b), using the pure H II spectrum of M17 to fit the strong VSG continuum in starbursts (Cesarsky et al., 1996b), an isolated PDR spectrum of the reflection nebula NGC 7023 (Cesarsky et al., 1996a) and the nuclear spectrum of Centaurus A representing the hot AGN spectrum (Laurent et al., 2000). Such diagnostics are extremely valuable for assessing the fuelling mechanisms of ambiguous sources such as ULIGs (Laurent et al., 2000; Tran et al., 2001) and can reveal the presence of obscured AGN in the mid-infrared. This diagnostic tool is most successful when used with spectra of high signal-to-noise and with sufficient coverage of the mid-infrared range [i.e. to best determine the continua shortward ($<5\mu\text{m}$)

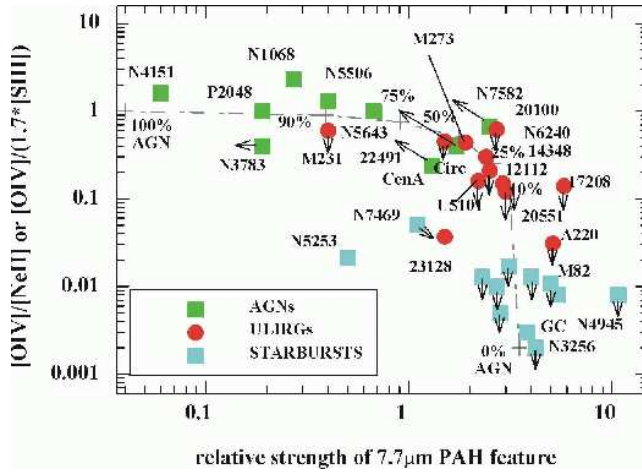


Fig a

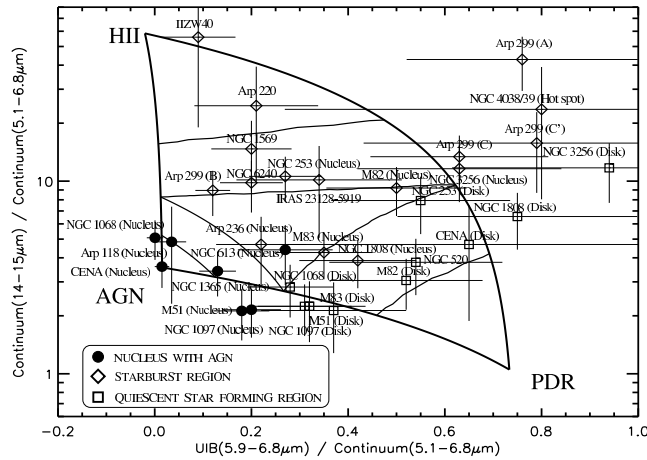


Fig b

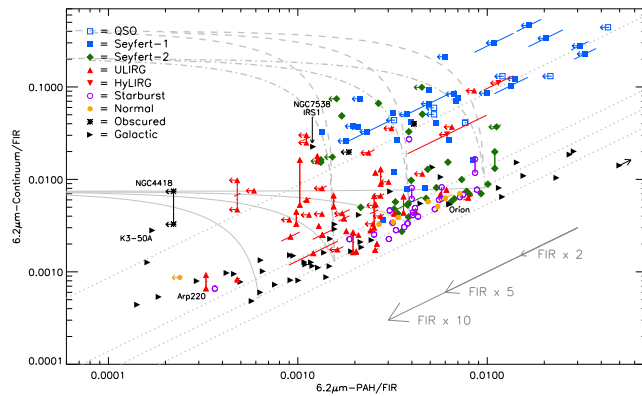


Fig c

Figure 5. UIB diagnostics from Genzel et al. (1998) (a) and Laurent et al. (2000) (b). Both of these diagrams show the mixing levels of starbursts and AGN in active sources. Finally the MIR/FIR diagnostic of Peeters et al. 2004 is shown for comparison (c).

and longward ($>12\mu\text{m}$) of the family of strong UIB features] that enables accurate decomposition of the H II PDR and AGN templates and reduces problems associated with blended mid-infrared absorption and emission lines (Spoon et al., 2002). A follow up of this method, on a larger sample of galaxies was presented by Peeters et al. (2004) with similar results. The authors also construct a new mid- and far-infrared combined diagnostic that is useful for differentiating obscured sources (Fig. 5c). In integrated galaxy spectra, where no spatial information is available, e.g. for compact and/or distant sources, decomposition of the spectral characteristics is the only means to identify the power sources constituting the mid-infrared emission (e.g. Vigroux, 1997, Rigopoulou et al., 1999; Lutz et al., 1998b; Mouri et al., 1998; Genzel et al., 1998; Laurent et al., 2000).

6.1.3. *Limitations*

The use of the UIB strength as a diagnostic has several limitations. One originates from the fact that measuring the strength of the $7.7\mu\text{m}$ UIB feature in the wavelength range of *ISOPHOT-S* ($2-11\mu\text{m}$) was challenging as ULIGs also display strong silicate absorption at $9.7\mu\text{m}$ and tracing the continuum was often extinction dependent. Another limitation of relying on UIB strength originates from its sensitivity to the radiation environment. Its absence in hard radiation fields in the vicinity of massive stars or AGN weakens its effectiveness as a tracer of star formation. Finally, as discussed by Laurent et al. (1999, 2000), *ISO*'s limited spatial resolution in the mid-infrared, may introduce a scatter into the diagnostic diagram, especially for distant sources with angular size smaller than the instrument beams. This results in a dilution of the AGN signatures as a larger fraction of the circumnuclear star forming regions of the host galaxy disk enter into the beam. For these reasons, while UIB diagnostics were relatively successful in particular for faint sources. The diagnostics formed purely from fine structure lines, which directly trace differing excitation regions within galaxies, offer far cleaner and more effective means of source-type segregation and should be preferred for classification of faint and high-redshift galaxies that will be observed by future telescopes.

6.1.4. *Broad-band colour diagnostics*

The well known diagnostics based on the broad band infrared colours determined from *IRAS* data (e.g. the *IRAS* $60\mu\text{m}/25\mu\text{m}$ colour represented the warm/cold emission ratio) have been extended to include *ISO* photometry (Spinoglio et al., 2002) and show the separation of 'warm' AGN (Sect. 5.2), 'cold' starburst (Sect. 4) and 'very cold' (Sect. 3) dust dominated systems (see their Fig. 14). While in the far-infrared,

the SEDs of Sey 1s and 2s are indistinguishable, the diagram of Spinoglio et al. (2002) is based on the fact that the SEDs of Sey1s are flatter in the mid- to far-infrared than Sey 2s. Using averaged spectra from this sample, the authors were able to produce redshift tracks on colour-colour diagrams for the Spitzer MIPS and IRAC filters as a means of determining infrared photometric redshifts. Even though these tracks were calculated without evolutionary considerations, the diagrams are useful tools to differentiate AGN (Seyfert 1 & 2s, QSOs) dominated sources from starbursts.

6.2. THE NATURE OF ULIGS

Using these techniques, the majority of ULIGs are found to be predominantly powered by starbursts. For large samples of ULIGs Lutz et al. (1998b), Rigopoulou et al. (1999) and Tran et al. (2001) corroborate the early result of (Genzel et al., 1998) and find that $\sim 75\text{-}85\%$ of their sample do not contain energetically dominant AGN. Starburst activity can explain the bulk of the bolometric luminosity although the presence of a weak or heavily obscured AGN cannot be excluded. While the fraction of AGN dominated sources is 15-25%, the fraction of AGN *hosting* ULIGs is 20-25%. The AGN dominated sources have ‘warm’ *IRAS* colours ($S_{25}/S_{60} \gtrsim 0.2$) confirming previous *IRAS* results on ULIGs with optical or near-infrared spectroscopic classification. Moreover, a comparison of the mid-infrared classification with good quality optical spectroscopy is remarkably consistent providing both optically classified H II regions and LINERs are both ascribed to the mid-infrared starburst class (Lutz et al., 1999).

6.3. THE NATURE OF LINERs

The nuclei of a large fraction (as much as one-third) of local galaxies display spectra with weak emission lines of lower ionisation than is seen in typical AGN, e.g. Seyfert nuclei. Furthermore, the low ionisation species present can not be explained through photoionisation by normal stars. The population of low ionisation nuclear emission-line regions - LINERs (Heckman, 1980) is well known to be mixed. Because of their prevalence, establishing the fraction of AGN or star-forming like LINERs has strong implications on our understanding of galaxies. *ISO* spectroscopic results clearly indicate that, at least in the infrared, their properties are more similar to starbursts (Lutz et al., 1999). In this case, the low ionisation emission lines are ascribed to ionising shocks related to starburst driven winds (Lutz et al., 1999; Sugai and Malkan, 2000). Interestingly though, in an infrared study of LINERs, Satyapal et al. (2004) found as much as two-thirds of the sample with hard

X-ray counterparts have compact X-ray morphologies consistent with those found for AGN. The remainder with scattered X-ray emission are brighter in the infrared than the compact ones. The authors found that most LINERs displaying high excitation mid-infrared lines also show compact X-ray morphology, even though a few systems deviate from this (i.e. NGC 404 and NGC 6240). These studies indicate that infrared bright LINERs are most likely members of a shock-dominated population whereas optical selection may trace the low luminosity AGN component. The fact that LINERs occupy a locus in ionisation diagrams situated between classical starbursts and AGN suggests an evolutionary connection whereby LINERs may represent a phase when the AGN is deeply buried and the unrelated starburst dominates the detected emission (Lutz et al., 1999).

6.4. ULIG SEDs

An alternative classification method arises from an analysis of ULIG SEDs that include *ISO* data. This includes fainter and/or more luminous ULIGs and HyLIGs that were inaccessible to *ISO*'s spectrometers. Often in conjunction with multi-wavelength data from other telescopes, *ISO* data has enabled classification of ULIGs through decomposition of their SEDs. A statistical study of 20 ULIGs (Klaas et al., 2001) clearly showed a progression of SED shapes. These were broadly divided into two types. The first (type A) show a power law increase from 1 to $50\mu\text{m}$ and are classified as Seyferts from optical spectroscopy. They also have warm infrared colours ($f_{25\mu\text{m}} / f_{60\mu\text{m}} > 0.2$). Type B sources display a relatively flat SED from 1 to $10\mu\text{m}$, that is followed by a steep rise towards the peak of emission in the far-infrared. These SED characteristics are displayed by ULIGs with optical spectroscopic classifications of Seyfert 2, LINER, H II/starburst. These are 'cool' ULIGs with infrared colour $f_{25\mu\text{m}} / f_{60\mu\text{m}} < 0.2$. The grouping of LINERs in the 'cool'-starburst-like ULIG class is consistent with the analysis of mid-infrared versus optical spectroscopic classification performed by Lutz et al. (1999) discussed in the previous section. This, together with the near-infrared colours (see Figure 6 in Klaas et al. (2001)) of ULIGs, suggest that the far-infrared emission from LINER-ULIGs is of starburst origin. Klaas et al. (2001) interpreted the emission of 'warm'-ULIGs (type A) to arise from dust heated to high temperatures directly from the central AGN, which in turn dominates the mid-infrared emission. The second SED feature is ascribed due to thermal re-radiation by dust heated by starburst activity. The indistinguishable far-infrared SEDs of AGN- and starburst-dominated ULIGs suggests that the far-infrared emission largely comes from less active or shielded regions that

are generally not heated by the AGN (Klaas et al., 2001). Thus Klaas et al. (2001) proposed a three-stage dust model consisting of hot AGN heated dust, warm starburst heated dust ($50\text{K} > T > 30\text{K}$) and cold, pre-starburst or cirrus like dust ($30\text{K} > T > 10\text{K}$). The general consensus from *ISO* spectroscopic results of warm ULIGs being AGN-dominated and cold ULIGs starburst-dominated is corroborated by the findings of Klaas et al. (2001).

6.5. HYLIGS AND THE INCREASING ROLE OF AGN AT HIGH LUMINOSITY

The increasing importance of AGN with increasing luminosity (Shier et al., 1996; Veilleux et al., 1997) has been confirmed by *ISO* observations of ULIGs (Lutz et al., 1998b; Tran et al., 2001; Charmandaris et al., 2002). Tran et al. (2001) quantified that the change from starburst- to AGN-dominated systems occurs at $\log_{10}(L_{IR}) \sim 12.4-12.5 L_{\odot}$. While *ISO* results show that $10^{12} L_{\odot}$ can be powered by star formation alone (Genzel et al., 1998; Lutz et al., 1998b; Rigopoulou et al., 1999; Tran et al., 2001), beyond $10^{13} L_{\odot}$ an AGN contribution seems inevitable. Moreover, the production of such a luminosity would require star formation rates $\gtrsim \text{few} \times 10^3 M_{\odot} \text{yr}^{-1}$. Such rates require huge concentrations of molecular gas to be present (most likely the result of mergers) and highly ineffective negative feedback (Takagi et al., 2003).

The prevalence of AGN in HyLIG samples partially arises from a selection effect. These rare luminous sources have been discovered with heterogeneous selection methods, most commonly through a correlation of known quasar or radio catalogues with *IRAS* or *ISO* surveys resulting in the known population being biased towards AGN. Constraining the properties of this sample and full consideration of the biases involved is unfortunately not possible due to the paucity of known HyLIGs. Nevertheless *ISO* observed several hyperluminous galaxies in a range of programs.

Only a few HyLIGs were sufficiently bright to permit low resolution spectroscopic observations. Analyses of IRAS 09104+4109 (Tran et al., 2001) and IRAS F15307+3252 (Aussel et al., 1998) showed that the mid-infrared emission predominantly originates from very compact regions $< 100\text{pc}$ (Taniguchi et al., 1997) with lower limits on the size of the emission region of 6pc for F15307 (Aussel et al., 1998) and $5/\sqrt{m}$ (m =magnification) for the Cloverleaf. These quasars show hot gas at temperatures in excess of 400K. They exhibit low UIB-to-continuum ratios expected for AGN. For F15307 SED modelling showed that a starburst component is required to fit this source fuelling 45% of its luminosity, although this poses a problem for the non-detection of CO

(Verma et al., 2002). In a sample of four HyLIGs including HyLIGs without clear AGN features, a SED analysis indicated an AGN was required to explain the IRAS-ISO SEDs (Verma et al., 2002). One of the highest redshift sources observed by *ISO* was the powerful radio galaxy 8C 1435+635 ($z=4.25$). It was shown to be hyperluminous and massive but the infrared-mm emission was solely ascribed to star formation and extremely high star formation rates were implied (Ivison et al., 1998).

Several HyLIGs are also well known PG quasars that do not conform to being dust free naked quasars (Haas et al., 2000b). Haas et al. (2003) show a schematic view of the evolution of SEDs encompassing various types. A significant AGN contribution is seen but PG quasars lack the cooler extended dust component seen in lower luminosity sources. Patchy or clumpy disk torus models may explain all of the far-infrared emission, without invoking starburst contributions.

6.6. STARBURST COMPONENTS IN AGN-HOSTING GALAXIES

Is concurrent star formation a requisite to explain the SEDs of QSOs displaying a far-infrared excess? Even the cold far-infrared-sub-mm emission of AGN dominated sources may be fuelled by the central obscured active nuclei itself. While *ISO* data cannot spatially resolve such emission, invoking strong star formation is not always necessary to describe the SEDs of AGN and ultraluminous quasars (see below). A clumpy distribution of obscuring material around the black hole allows high energy photons to escape and heat extended dust (Nenkova et al. (2002), Elitzur et al. (2003)). Alternatively warped, thick and extended disks (on parsec scales) have been proposed to explain the emission (e.g. Granato and Danese (1994)).

There is clear evidence that some AGN do not host bolometrically important starbursts. For example, the archetypal Seyfert 2 galaxy NGC5252, shows no signs for starburst activity and the bulk of its far-infrared SED can be explained by the heating of the cold dust by the general ISRF while a small fraction is ascribed to a very large disk (kpc scale) surrounding the active nucleus (Prieto and Acosta-Pulido, 2003). The infrared emission of narrow-line Seyfert 1 galaxies measured by *ISOPHOT* can be accounted for by re-radiation of the soft X-ray component (Polletta and Courvoisier, 1999a; Polletta and Courvoisier, 1999b). Similarly, at higher AGN power, starburst activity is not a necessary requisite to explain the full SEDs of a large sample of 3CR sources (Siebenmorgen et al., 2004a) or PG quasars (Haas et al., 2000b; Haas et al., 2003) for which AGN heating plus extended cold dust suffices (also see Rocca-Volmerange and Remazeilles, 2005). In a sample of 22 quasars, starburst emission does contribute to the far-

infrared emission but to a level no more than 27% (Polletta et al., 2000).

Thus while concurrent starbursts may be present, *ISO* SEDs of optically classified AGN and quasars indicate that they are typically not bolometrically dominant. The detection of spatially resolved starburst tracers in the host galaxies of quasars or AGN-like ULIGs and HyLIGs would clarify this issue.

6.7. AGN COMPONENTS IN STARBURST-DOMINATED GALAXIES

Infrared diagnostics were largely successful in assessing the nature of most infrared sources. However, how strong a limit can one place upon the absence of an AGN in the mid-infrared? At short mid-infrared wavelengths $< 10\mu\text{m}$ the strong VSG continuum related to the star-formation in starburst dominated sources will overshadow the weaker AGN continuum, particularly in Sey 2s where the continuum due to the AGN will suffer high obscuration (Laurent et al., 2000; Schulz et al., 2000). This results in an AGN being identified through the Laurent et al. (2000) diagnostic only if it dominates over star formation. Galaxies such as IRAS 00183-7111 and Arp 220 are highly obscured even in the mid-infrared (Sturm et al., 1996; Tran et al., 2001; Spoon et al., 2004), Arp 220 may be optically thick even in the far-infrared (Fischer et al., 1997; Haas et al., 2001; González-Alfonso et al., 2004)). This substantial obscuration by dust may cause any AGN to be completely hidden (Schulz et al., 2000), a fact which is compounded by the possibility that AGN tracers could in some cases be completely overshadowed by circumnuclear activity (Laurent et al., 1999; Dennefeld et al., 2003). Without spatial resolution, the possibility of detecting extremely obscured or weak AGN in, at least the mid-infrared, appears to be low (Laurent et al., 2000; Schulz et al., 2000).

6.8. NEWLY DETECTED ULIGS

As well as the ULIGs and HyLIGs described here which were known prior to the launch of *ISO*, several were discovered primarily in *ISO* surveys. Among the many ULIGs detected in the deep *ISO* surveys, a hyperluminous QSO (Morel et al., 2001) was discovered in ELAIS, and a highly extinguished ($A_V \sim 1000$) gas and dust rich elliptical was detected in the *ISOPHOT* Serendipitous Survey (Krause et al., 2003). One might expect the population of heavily obscured extremely red objects (EROs) to be luminous in the infrared. Indeed, ultraluminous emission (and high star formation rates) was determined from the *ISO* SEDs of the ERO HR10 with a SED similar to that of Arp220 (Elbaz et al., 2002) and a sub-mJy radio ERO from the Phoenix survey

(where coeval star formation and AGN are probable (Afonso et al., 2001)) through targeted observations. Tentative infrared detections of a gamma ray burst were also reported to be at ULIG luminosities (Hanlon et al., 1999; Hanlon et al., 2000) originating from either the host galaxy or the GRB infrared afterglow.

6.9. EVOLUTION OF ULIGS

The basic similarity in luminosity and space density of ULIGs and quasars, and the fact that unbiased samples of ULIGs contained both star forming and AGN members, led to the suggestions that the two populations are linked through evolution (Sanders et al. (1988), also see Sanders and Mirabel (1996) and references therein). The example of the composite galaxy NGC 985 is used to discuss possible ULIG formation and destruction scenarios (Appleton et al., 2002). Some popular evolutionary models include the following that were recently well summarised by L ipari et al. (2003):

- (1) merger - giant shocks - super-starbursts + galactic winds - elliptical galaxies (Joseph, 1999)
- (2) merger - H₂ inflow (starbursts) - cold ULIRGs - warm ULIRGs+QSOs - optical QSOs (Sanders, 1999)
- (3) merger/s - extreme starburst + galactic wind (inflow + outflow) - FeII/BAL composite IR-QSOs - standard QSOs and ellipticals (L ipari et al., 2003)

6.9.1. Merger Stage and Luminosity

Merging activity that initiates associated starbursts leading to the ultraluminous behaviour in the early stages is common to all of the scenarios above. Thus the merger stage should be related to the luminosity evolution of ULIGs. Furthermore, if quasars are the end product of ULIG evolution and the merger stage indicates an evolutionary status, then more advanced mergers should appear more AGN-like.

The near- to mid-infrared energy distributions of ULIGs are dominated by compact nuclear regions (Charmandaris et al., 2002). This confirms results from high resolution ground-based observations (Soifer et al., 2000) that show 30-100% of the mid-infrared flux can be accounted for by the central 100-300pc. Based on *ISO* imaging of a merging sequence of active galaxies, including starbursts, LIGs and ULIGs, Charmandaris et al. (2001a) suggest an evolutionary sequence that is traced by the 15 μ m/7 μ m colour that monotonically increases with star formation activity, from 1 (quiescent) to 5 (extreme), as galaxies evolve from pre-starburst to the merging starburst phase. The ratio

decreases again to 1 for the post starburst phase in evolved merger remnants [cf local less luminous post-starburst colours of NGC 7714 (O’Halloran et al., 2000) and NGC 1741 (O’Halloran et al., 2002)] The fact that the extra-nuclear activity typically contributes only a minor fraction to the bolometric luminosity of ULIGs (in comparison to LIGs (Hwang et al., 1999)) implies that simple scaling in mass and luminosity does not link the two populations, but evolutionary differences (such as merger stage, or presence of an AGN) could play a role. It is unclear whether this hardening of the mid-infrared continuum is due to an AGN contribution. The amount of molecular gas may also affect the spectral feature differences seen between the populations, such as the presence of ice features (Spoon et al., 2002). Increasing compactness of sources with increasing merger stage shown by Hwang et al. (1999) implies that compact ULIGs are in a more advanced merger state than LIGs.

However, based upon a comparison of the NIR morphologies of merging ULIGs and infrared spectroscopic tracers, Lutz et al. (1998b) and Rigopoulou et al. (1999) do not find any relation of increasing AGN-like activity with merger stage. In addition ULIGs appear to not show a trend of increasing luminosity with merger stage again contrary to expectations of these evolutionary scenarios (Rigopoulou et al., 1999). Indeed Rigopoulou et al. (1999) suggest that early merger stage ULIGs may be exhibiting maximal luminosities (also see Murphy et al., 2001). Moreover, the mass of the warm, cold and very cold dust components found in ULIG SEDs show no relation to merger stage (Klaas et al., 2001). The evolution or merger-stage may not be traced well simply by nuclear separation alone as a merger stage indicator. More complex differences in the mass distribution and dynamics of ULIGs more likely influence the luminosity and appearance of AGN.

6.9.2. *Dust evolution in quasars*

If ULIGs are related to quasars as the dust obscured members of that class, understanding the dust properties of quasars also serve to test the evolutionary connections between quasars and ULIGs. In the Sanders et al. (1988) scenario a quasar is preceded by a dusty ULIG-phase and as a result it is unlikely that the obscuring dust will suddenly disappear, some traces in the infrared should remain. Haas et al. (2003) investigated a sample of 64 PG quasars and identified a range of SED shapes that could mark a transition between states. The SED analysis showed that the central regions of PG quasars suffer low extinction ($A_V < 0.3$) with an optical slope α_{opt} that is independent of infrared properties like the near- to mid-infrared slope α_{IR} . Therefore, with regard to the unification schemes a nearly face-on view onto the PG

quasars was assumed. The observed variety of SEDs were grouped into physically meaningful classes, that reflect the amount and distribution of the reprocessing dust around the AGN according to evolution of the quasar (Haas et al., 2003). Their new evolutionary scenario begins with dissipative cloud-cloud collisions and angular momentum constraints that create the organisation of dust clouds into a torus/disk like configuration. Starburst activity is initiated giving rise to a far-infrared bump but it becomes increasingly overpowered by the central AGN which results in increasing mid-infrared emission and steepening of the mid- to far-infrared spectral slope. As the AGN continues to grow, the mid-infrared remains high and the mid- to far-infrared slope decreases until the black hole begins to starve and a decline in the mid-infrared and far-infrared emission is observed. Figure 12 in Haas et al. (2003) depicts this scheme, the SEDs are arranged along the expectations for such an evolutionary scheme.

6.9.3. *Relation of broad absorption line quasars to ULIGs*

Broad absorption line quasars are a rare class of the optically selected quasar population ($\sim 12\%$) but have a higher frequency in far-infrared luminous, strong FeII and weak [OIII] emission line selected samples. Both orientation and age arguments are consistent with the origin of the broad absorption features with no clear resolution which is the most likely cause. Elvis (2000) suggest the broad absorption arises from viewing a single funnel-shaped outflow of absorbing material directly down the flow. It has also been proposed that these sources are quasars viewed at an orientation directly along the radial surface of the torus, where winds along the surface give rise to the observed absorption. Alternatively they may be a young phase in quasar evolution. The latter together with the high occurrence of BALQSO in *IRAS* selected samples suggests that they may be a transition stage between ULIGs and QSOs (Voit et al., 1993; Lípari, 1994; Egami et al., 1996; Canalizo and Stockton, 2001; Lípari et al., 2003). In this scenario very young QSOs are ejecting their gaseous envelopes at very high velocity close to the initiation of the active phase of the black hole (Hazard et al., 1984).

Two BALQSOs were serendipitously discovered in *ISO* surveys: the FeLoBAL² ISO J005645.1-273816 was discovered in an ISOCAM distant cluster survey (Duc et al., 2002). 00 37 14.3 -42 34 55.6 was discovered in ELAIS (Alexander et al., 2001). For the former, high absorption and hot dust emission are implied by the high mid-infrared to UV ratio which may indicate the mid-infrared is an efficient means

² FeLoBALs show absorption lines from many excited states of Fe II and having low ionisation lines and are heavily absorbed in X-rays

to detect LoBALQSOs (Duc et al., 2002). The sources 00 37 14.3 -42 34 55.6 was the only BALQSO then known to have both infrared and hard X-ray detections. While it has a similar hard X-ray/MIR flux ratio to high redshift quasars, it differs from low-redshift BALQSOs. Alexander et al. attribute this to absorption. As a consequence they suggest that absorbed BALQSOs at high redshift should be easily detected in the hard X-ray bands. In addition the only radio-loud BALQSO known, 1556+3517, was observed to investigate the relation between radio-loud quasars and the BALQSO phenomenon. Mid-infrared detections implied $4M_{\odot}$ of dust lie along the line of sight which most likely arises from the molecular torus, the NLR, or a recent starburst rather than from the BALQSO wind itself (Clavel, 1998). *ISO* data confirms that even in this diverse, small sample, the BALQSO phenomenon and obscuration (i.e. infrared emission) are connected. L ipari et al. (2003) speculate on an evolutionary connection between BALQSOs and ULIGs.

6.10. SUMMARY

Evaluating which of the three scenarios mentioned earlier in this Section is most realistic will continue to be addressed by future missions. However, the *ISO* results clearly suggest that a simple Sanders et al. (1988) evolutionary scenario of a merger triggered starburst event with an evolving obscured- naked quasar scenario to be unlikely. Rather, it seems that the nature of the diverse infrared luminous ULIGs and HyLIGs has a far more complex history. Whether a starburst or an AGN dominates the bolometric luminosity of a ULIG is most probably determined by local conditions, evolution and obscuration by dust. Nearby ULIGs are mostly starburst dominated systems with ‘cold’ colours. This cold fraction decreases at higher luminosities where AGN contributions become prevalent and galaxy SEDs are ‘warmer’. ULIGs are often linked to high-redshift ($z\sim 2$) (sub-)mm emitting galaxies which comprise a significant fraction of the infrared background and contribute significantly to the star formation density at that epoch. If ULIGs and sub-mm galaxies are members of the same population then strong evolution is implied since the locally unimportant ULIGs, that constitute less than 1% of the local star-formation density, must dominate the infrared number counts at higher redshifts (Elbaz and Cesarsky, 2003). The strongly evolving $z\lesssim 1.5$ LIGs discovered in *ISO-CAM* surveys (see Elbaz et al. and Oliver et al. in this volume) that resolve 10-60% of the far-IR-sub-mm background may provide a step between.

7. Active Galaxies as seen by ISO: a summary

The Infrared Space Observatory has produced a wealth of information regarding the infrared emission properties of the full range of active galaxies. Greatly enhancing the IRAS legacy, it has provided a physical basis upon which the next generation of infrared telescopes such as Spitzer, SOFIA, ASTRO-F and Herschel will build. Most of *ISO*'s power was due to the improved sensitivity and extended wavelength coverage. The addition of high resolution spectroscopy and development of new diagnostic diagrams have enabled us to probe the ongoing physical conditions of the ISM in active galaxies and to quantitatively assess the presence and bolometric contribution of star formation or an AGN in infrared luminous sources. Analysis of fine structure lines provided an excellent set of diagnostic tools that will be better populated and applied to a wider variety of sources in future missions with even higher sensitivity. The weakness of the sulphur fine structure lines in starburst galaxies and of the cooling line [CII]158 μ m in the most luminous active galaxies suggests that other strong lines (e.g. [NeII]12.8 μ m) should be the preferred indicators of star forming objects. The finding of *IRAS* that galaxies with "cold" infrared colours are starburst dominated and "warm" are AGN dominated was broadly confirmed with the new *ISO* data. Although, it was shown that spatially resolved spectroscopic information is necessary to address the issue of the origin of the far-infrared emission in AGN and the role of concurrent star formation. *ISO* results on AGN in general support unification scenarios, but suggest that a clumpy distribution of obscuring material around the active nucleus may be a better representation than the commonly assumed torus. While the majority of ULIGs are starburst dominated, it now appears that an increasing fraction of AGN at higher infrared luminosities is present. Mergers are indeed the trigger of ULIG activity, but the simple generic evolution of a luminous system from a ULIG to an optical-QSO phase appears unlikely with more local factors influencing the presence of an AGN. With increases in sensitivity and spatial resolution, it is certain that the suite of current and forthcoming infrared telescopes will enhance our knowledge of the obscured active universe by probing fainter and to higher redshifts as well as in more spatial detail.

Acknowledgements

We would like to thank Matthias Tecza for his comments on this text. We are also grateful to Eckhard Sturm for providing the SWS+LWS

spectra shown in Figure 1 and for discussion. This work was supported by the DLR grant FKZ: 50QI 0202.

References

- Acosta-Pulido, J. A., U. Klaas, R. J. Laureijs, B. Schulz, U. Kinkel, P. Abraham, H. O. Castaneda, L. Cornwall, C. Gabriel, I. Heinrichsen, U. Herbstmeier, H. Krueger, and G. Pelz: 1996. *A&A* **315**, L121–L124.
- Afonso, J., B. Mobasher, B. Chan, and L. Cram: 2001. *ApJ* **559**, L101–L104.
- Alexander, D. M., A. Efstathiou, J. H. Hough, D. K. Aitken, D. Lutz, P. F. Roche, and E. Sturm: 1999a. *MNRAS* **310**, 78–86.
- Alexander, D. M., F. La Franca, F. Fiore, X. Barcons, P. Ciliegi, L. Danese, R. Della Ceca, A. Franceschini, C. Gruppioni, G. Matt, I. Matute, S. Oliver, F. Pompilio, A. Wolter, A. Efstathiou, P. Héraudeau, G. C. Perola, M. Perri, D. Rigopoulou, M. Rowan-Robinson, and S. Serjeant: 2001. *ApJ* **554**, 18–26.
- Alexander, D. M., M. Ruiz, and J. H. Hough: 1999b. In: *ESA SP-435: Workshop on ISO Polarisation Observations*. pp. 1–+.
- Alexander, T., D. Lutz, E. Sturm, R. Genzel, A. Sternberg, and H. Netzer: 2000. *ApJ* **536**, 710–717.
- Alexander, T., E. Sturm, D. Lutz, A. Sternberg, H. Netzer, and R. Genzel: 1999c. *ApJ* **512**, 204–223.
- Allamandola, L. J., S. A. Sandford, D. M. Hudgins, and F. C. Witteborn: 1995. In: *ASP Conf. Ser. 73: From Gas to Stars to Dust*. pp. 23–32.
- Allamandola, L. J., A. G. G. M. Tielens, and J. R. Barker: 1985. *ApJ* **290**, L25–L28.
- Alonso-Herrero, A., A. C. Quillen, C. Simpson, A. Efstathiou, and M. J. Ward: 2001. *AJ* **121**, 1369–1384.
- Alton, P. B., M. Trewhella, J. I. Davies, R. Evans, S. Bianchi, W. Gear, H. Thronson, E. Valentijn, and A. Witt: 1998. *A&A* **335**, 807–822.
- Andreani, P., R. A. E. Fosbury, I. van Bemmel, and W. Freudling: 2002. *A&A* **381**, 389–400.
- Antón, S., A. H. C. Thean, A. Pedlar, and I. W. A. Browne: 2002. *MNRAS* **336**, 319–327.
- Antonucci, R.: 1993. *ARA&A* **31**, 473–521.
- Appleton, P. N., V. Charmandaris, Y. Gao, F. Combes, F. Ghigo, C. Horellou, and I. F. Mirabel: 2002. *ApJ* **566**, 682–698.
- Appleton, P. N., V. Charmandaris, C. Horellou, I. F. Mirabel, F. Ghigo, J. L. Higdon, and S. Lord: 1999. *ApJ* **527**, 143–153.
- Appleton, P. N., V. Charmandaris, C. Horellou, I. F. Mirabel, and O. Laurent: 2000. *LNP Vol. 548: ISO Survey of a Dusty Universe* pp. 232–+.
- Appleton, P. N. and C. Struck-Marcell: 1996. *Fundamentals of Cosmic Physics* **16**, 111–220.
- Aussel, H., M. Gerin, F. Boulanger, F. X. Desert, F. Casoli, R. M. Cutri, and M. Signore: 1998. *A&A* **334**, L73–L76.
- Baluteau, J., F. Damour, E. Caux, C. Gry, and C. Caccarelli: 2003. In: *ESA SP-511: Exploiting the ISO Data Archive. Infrared Astronomy in the Internet Age*. pp. 209–+.
- Barger, A. J., L. L. Cowie, and E. A. Richards: 2000. *AJ* **119**, 2092–2109.
- Barthel, P. D.: 1989. *ApJ* **336**, 606–611.

- Beichman, C. A.: 1987. *ARA&A* **25**, 521–563.
- Beichman, C. A., G. Neugebauer, H. J. Habing, P. E. Clegg, and T. J. Chester: 1988. In: *NASA RP-1190, Vol. 1 (1988)*. pp. 0–+.
- Bendo, G. J., R. D. Joseph, M. Wells, P. Gallais, M. Haas, A. M. Heras, U. Klaas, R. J. Laureijs, K. Leech, D. Lemke, L. Metcalfe, M. Rowan-Robinson, B. Schulz, and C. Telesco: 2003. *AJ* **125**, 2361–2372.
- Bergvall, N., J. Masegosa, G. Östlin, and J. Cernicharo: 2000. *A&A* **359**, 41–50.
- Bertone, E., G. Tagliaferri, G. Ghisellini, A. Treves, P. Barr, A. Celotti, M. Chiaberge, and L. Maraschi: 2000. *A&A* **356**, 1–10.
- Binette, L., A. S. Wilson, A. Raga, and T. Storchi-Bergmann: 1997. *A&A* **327**, 909–920.
- Block, D. L. and M. Sauvage: 2000. *A&A* **353**, 72–76.
- Boselli, A., J. Lequeux, A. Contursi, G. Gavazzi, O. Boulade, F. Boulanger, D. Cesarsky, C. Dupraz, S. Madden, M. Sauvage, F. Viallefond, and L. Vigroux: 1997. *A&A* **324**, L13–L16.
- Boselli, A., J. Lequeux, M. Sauvage, O. Boulade, F. Boulanger, D. Cesarsky, C. Dupraz, S. Madden, F. Viallefond, and L. Vigroux: 1998. *A&A* **335**, 53–68.
- Boulade, O., M. Sauvage, B. Altieri, J. Blommaert, P. Gallais, S. Guest, L. Metcalfe, K. Okumura, S. Ott, D. Tran, and L. Vigroux: 1996. *A&A* **315**, L85–L88.
- Boulanger, F., A. Abergel, J. P. Bernard, D. Cesarsky, J. L. Puget, W. T. Reach, C. Ryter, C. J. Cesarsky, M. Sauvage, D. Tran, L. Vigroux, E. Falgarone, J. Lequeux, M. Perault, and D. Rouan: 1998a. In: *ASP Conf. Ser. 132: Star Formation with the Infrared Space Observatory*. pp. 15–+.
- Boulanger, F., P. Boissel, D. Cesarsky, and C. Ryter: 1998b. *A&A* **339**, 194–200.
- Bradford, C. M., G. J. Stacey, J. Fischer, H. A. Smith, R. J. Cohen, M. A. Greenhouse, S. D. Lord, D. Lutz, R. Maiolino, M. A. Malkan, and N. Q. Rieu: 1999. In: *ESA SP-427: The Universe as Seen by ISO*. pp. 861–+.
- Brauher, J. and S. Lord: 2000. *Bulletin of the American Astronomical Society* **32**, 1286–+.
- Brauher, J., S. Lord, S. Unger, M. Wolfire, and J. Fischer: 1997. *Bulletin of the American Astronomical Society* **29**, 1246–+.
- Calzetti, D., L. Armus, R. C. Bohlin, A. L. Kinney, J. Koornneef, and T. Storchi-Bergmann: 2000. *ApJ* **533**, 682–695.
- Canalizo, G. and A. Stockton: 2001. *ApJ* **555**, 719–743.
- Cesarsky, D., J. Lequeux, A. Abergel, M. Perault, E. Palazzi, S. Madden, and D. Tran: 1996a. *A&A* **315**, L309–L312.
- Cesarsky, D., J. Lequeux, A. Abergel, M. Perault, E. Palazzi, S. Madden, and D. Tran: 1996b. *A&A* **315**, L305–L308.
- Charmandaris, V., F. Combes, and J. M. van der Hulst: 2000. *A&A* **356**, L1–L4.
- Charmandaris, V., O. Laurent, E. Le Floch, I. F. Mirabel, M. Sauvage, S. C. Madden, P. Gallais, L. Vigroux, and C. J. Cesarsky: 2002. *A&A* **391**, 429–440.
- Charmandaris, V., O. Laurent, I. F. Mirabel, and P. Gallais: 2001a. *Astrophysics and Space Science Supplement* **277**, 55–58.
- Charmandaris, V., O. Laurent, I. F. Mirabel, P. Gallais, M. Sauvage, L. Vigroux, and C. Cesarsky: 2001b. *Ap&SS* **276**, 553–559.
- Charmandaris, V., O. Laurent, I. F. Mirabel, P. Gallais, M. Sauvage, L. Vigroux, C. Cesarsky, and P. N. Appleton: 1999. *A&A* **341**, 69–73.
- Charmandaris, V., I. F. Mirabel, D. Tran, O. Laurent, C. J. Cesarsky, P. Gallais, M. Sauvage, and L. Vigroux: 1997. In: *Extragalactic Astronomy in the Infrared*. pp. 283–+.

- Chiar, J. E., A. G. G. M. Tielens, D. C. B. Whittet, W. A. Schutte, A. C. A. Boogert, D. Lutz, E. F. van Dishoeck, and M. P. Bernstein: 2000. *ApJ* **537**, 749–762.
- Clavel, J.: 1998. *A&A* **331**, 853–856.
- Clavel, J., B. Schulz, B. Altieri, P. Barr, P. Claes, A. Heras, K. Leech, L. Metcalfe, and A. Salama: 2000. *A&A* **357**, 839–849.
- Colbert, J. W., M. A. Malkan, P. E. Clegg, P. Cox, J. Fischer, S. D. Lord, M. Luhman, S. Satyapal, H. A. Smith, L. Spinoglio, G. Stacey, and S. J. Unger: 1999. *ApJ* **511**, 721–729.
- Combes, F.: 2001. *Astrophysics and Space Science Supplement* **277**, 29–38.
- Contini, M., M. A. Prieto, and S. M. Viegas: 1998. *ApJ* **505**, 621–633.
- Contini, M., S. M. Viegas, and M. A. Prieto: 2002. *A&A* **386**, 399–414.
- Contursi, A., J. Lequeux, D. Cesarsky, F. Boulanger, M. Rubio, M. Hanus, M. Sauvage, D. Tran, A. Bosma, S. Madden, and L. Vigroux: 2000. *A&A* **362**, 310–324.
- Cox, P. P., P. R. Roelfsema, J. P. Baluteau, E. Peeters, L. Martin-Hernandez, A. G. G. M. Tielens, B. M. Swinyard, T. Lim, and M. F. Kessler: 1999. In: *ESA SP-427: The Universe as Seen by ISO*. pp. 631–+.
- Crowther, P. A., S. C. Beck, A. J. Willis, P. S. Conti, P. W. Morris, and R. S. Sutherland: 1999. *MNRAS* **304**, 654–668.
- Dale, D. A., G. Helou, J. R. Brauher, R. M. Cutri, S. Malhotra, and C. A. Beichman: 2004. *ApJ* **604**, 565–571.
- Dale, D. A., G. Helou, A. Contursi, N. A. Silbermann, and S. Kolhatkar: 2001a. *ApJ* **549**, 215–227.
- Dale, D. A., G. Helou, G. Neugebauer, B. T. Soifer, D. T. Frayer, and J. J. Condon: 2001b. *AJ* **122**, 1736–1746.
- Dale, D. A., N. A. Silbermann, G. Helou, E. Valjavec, S. Malhotra, C. A. Beichman, J. Brauher, A. Contursi, H. L. Dinerstein, D. J. Hollenbach, D. A. Hunter, S. Kolhatkar, K. Lo, S. D. Lord, N. Y. Lu, R. H. Rubin, G. J. Stacey, H. A. Thronson, M. W. Werner, and H. G. Corwin: 2000. *AJ* **120**, 583–603.
- Dartois, E., O. Marco, G. M. Muñoz-Caro, K. Brooks, D. Deboffle, and L. d’Hendecourt: 2004. *A&A* **423**, 549–558.
- Davies, J. I., P. Alton, M. Trewhella, R. Evans, and S. Bianchi: 1999. *MNRAS* **304**, 495–500.
- de Grijp, M. H. K., G. K. Miley, J. Lub, and T. de Jong: 1985. *Nature* **314**, 240–242.
- Dennefeld, M., T. Boller, D. Rigopoulou, and H. W. W. Spoon: 2003. *A&A* **406**, 527–534.
- Desert, F.-X., F. Boulanger, and J. L. Puget: 1990. *A&A* **237**, 215–236.
- Domingue, D. L., W. C. Keel, S. D. Ryder, and R. E. White: 1999. *AJ* **118**, 1542–1550.
- Domingue, D. L., J. W. Sulentic, and A. Durbala: 2005. *ArXiv Astrophysics e-prints*.
- Domingue, D. L., J. W. Sulentic, C. Xu, J. Mazzarella, Y. Gao, and R. Rampazzo: 2003. *AJ* **125**, 555–571.
- Downes, D. and P. M. Solomon: 1998. *ApJ* **507**, 615–654.
- Draine, B. T.: 2003. *ARA&A* **41**, 241–289.
- Draine, B. T. and A. Li: 2001. *ApJ* **551**, 807–824.
- Duc, P.-A., P. B. Hall, D. Fadda, P. Chaniel, D. Elbaz, P. Monaco, E. Pompei, B. M. Poggianti, H. Flores, A. Franceschini, A. Biviano, A. Moorwood, and C. Cesarsky: 2002. *A&A* **389**, L47–L50.
- Efstathiou, A., M. Rowan-Robinson, and R. Siebenmorgen: 2000. *MNRAS* **313**, 734–744.
- Egami, E., F. Iwamuro, T. Maihara, S. Oya, and L. L. Cowie: 1996. *AJ* **112**, 73–+.

- Elbaz, D. and C. J. Cesarsky: 2003. *Science* **300**, 270–274.
- Elbaz, D., H. Flores, P. Chanial, I. F. Mirabel, D. Sanders, P.-A. Duc, C. J. Cesarsky, and H. Aussel: 2002. *A&A* **381**, L1–L4.
- Elitzur, M., M. Nenkova, and Z. Ivezić: 2003. *ArXiv Astrophysics e-prints*.
- Elvis, M.: 2000. *New Astronomy Review* **44**, 559–562.
- Förster Schreiber, N. M., R. Genzel, D. Lutz, D. Kunze, and A. Sternberg: 2001. *ApJ* **552**, 544–571.
- Förster Schreiber, N. M., H. Roussel, M. Sauvage, and V. Charmandaris: 2004. *A&A* **419**, 501–516.
- Förster Schreiber, N. M., M. Sauvage, V. Charmandaris, O. Laurent, P. Gallais, I. F. Mirabel, and L. Vigroux: 2003. *A&A* **399**, 833–855.
- Fanti, C., F. Pozzi, R. Fanti, S. A. Baum, C. P. O’Dea, M. Bremer, D. Dallacasa, H. Falcke, T. de Graauw, A. Marecki, G. Miley, H. Rottgering, R. T. Schilizzi, I. Snellen, R. E. Spencer, and C. Stanghellini: 2000. *A&A* **358**, 499–513.
- Farrah, D., J. Afonso, A. Efstathiou, M. Rowan-Robinson, M. Fox, and D. Clements: 2003. *MNRAS* **343**, 585–607.
- Fischer, J.: 2000. In: *ESA SP-456: ISO Beyond the Peaks: The 2nd ISO Workshop on Analytical Spectroscopy*. pp. 239–+.
- Fischer, J., S. D. Lord, S. J. Unger, C. M. Bradford, J. R. Brauher, P. E. Clegg, J. W. Colbert, P. Cox, M. A. Greenhouse, V. Harvey, M. A. Malkan, G. Melnick, H. A. Smith, L. Spinoglio, V. Strelitski, and J. P. Suter: 1999a. In: *ESA SP-427: The Universe as Seen by ISO*. pp. 817–+.
- Fischer, J., M. L. Luhman, S. Satyapal, M. A. Greenhouse, G. J. Stacey, C. M. Bradford, S. D. Lord, J. R. Brauher, S. J. Unger, P. E. Clegg, H. A. Smith, G. Melnick, J. W. Colbert, M. A. Malkan, L. Spinoglio, P. Cox, V. Harvey, J.-P. Suter, and V. Strelitski: 1999b. *Ap&SS* **266**, 91–98.
- Fischer, J., S. Satyapal, G. Melnick, P. Cox, J. Cernicharo, M. L. Luhman, G. J. Stacey, H. A. Smith, S. D. Lord, and M. A. Greenhouse: 1997. *Bulletin of the American Astronomical Society* **29**, 1356–+.
- Freudling, W., R. Siebenmorgen, and M. Haas: 2003. *ApJ* **599**, L13–L16.
- Gallais, P., V. Charmandaris, E. Le Floch, I. F. Mirabel, M. Sauvage, L. Vigroux, and O. Laurent: 2004. *A&A* **414**, 845–855.
- Galliano, F., S. C. Madden, A. P. Jones, C. D. Wilson, J.-P. Bernard, and F. Le Peintre: 2003. *A&A* **407**, 159–176.
- Gao, Y., Q. D. Wang, P. N. Appleton, and R. A. Lucas: 2003. *ApJ* **596**, L171–L174.
- Gao, Y., C. Xu, N. Y. Lu, R. Tuffs, and J. Sulentic: 2001. *Bulletin of the American Astronomical Society* **33**, 835–+.
- Genzel, R., D. Lutz, E. Sturm, E. Egami, D. Kunze, A. F. M. Moorwood, D. Rigopoulou, H. W. W. Spoon, A. Sternberg, L. E. Tacconi-Garman, L. Tacconi, and N. Thatte: 1998. *ApJ* **498**, 579–+.
- Gillett, F. C., D. E. Kleinmann, E. L. Wright, and R. W. Capps: 1975. *ApJ* **198**, L65–L68.
- Giveon, U., A. Sternberg, D. Lutz, H. Feuchtgruber, and A. W. A. Pauldrach: 2002. *ApJ* **566**, 880–897.
- González-Alfonso, E., H. A. Smith, J. Fischer, and J. Cernicharo: 2004. *ApJ* **613**, 247–261.
- Gorjian, V., J. L. Turner, and S. C. Beck: 2001. *ApJ* **554**, L29–L32.
- Granato, G. L. and L. Danese: 1994. *MNRAS* **268**, 235–+.
- Haas, M.: 1998. *A&A* **337**, L1–L4.
- Haas, M., R. Chini, and U. Klaas: 2005. *A&A* **433**, L17–L20.

- Haas, M., R. Chini, K. Meisenheimer, M. Stickel, D. Lemke, U. Klaas, and E. Kreysa: 1998a. *ApJ* **503**, L109+.
- Haas, M., U. Klaas, and S. Bianchi: 2002. *A&A* **385**, L23–L26.
- Haas, M., U. Klaas, I. Coulson, E. Thommes, and C. Xu: 2000a. *A&A* **356**, L83–L87.
- Haas, M., U. Klaas, S. A. H. Müller, F. Bertoldi, M. Camenzind, R. Chini, O. Krause, D. Lemke, K. Meisenheimer, P. J. Richards, and B. J. Wilkes: 2003. *A&A* **402**, 87–111.
- Haas, M., U. Klaas, S. A. H. Müller, R. Chini, and I. Coulson: 2001. *A&A* **367**, L9–L13.
- Haas, M., D. Lemke, M. Stickel, H. Hippelein, M. Kunkel, U. Herbstmeier, and K. Mattila: 1998b. *A&A* **338**, L33–L36.
- Haas, M., S. A. H. Müller, F. Bertoldi, R. Chini, S. Egner, W. Freudling, U. Klaas, O. Krause, D. Lemke, K. Meisenheimer, R. Siebenmorgen, and I. van Bemmel: 2004. *A&A* **424**, 531–543.
- Haas, M., S. A. H. Müller, R. Chini, K. Meisenheimer, U. Klaas, D. Lemke, E. Kreysa, and M. Camenzind: 2000b. *A&A* **354**, 453–466.
- Hanlon, L., R. J. Laureijs, L. Metcalfe, B. McBreen, B. Altieri, A. Castro-Tirado, A. Claret, E. Costa, M. Delaney, M. Feroci, F. Frontera, T. Galama, J. Gorosabel, P. Groot, J. Heise, M. Kessler, C. Kouveliotou, E. Palazzi, J. van Paradijs, L. Piro, and N. Smith: 2000. *A&A* **359**, 941–947.
- Hanlon, L., L. Metcalfe, M. Delaney, R. Laureijs, B. McBreen, N. Smith, B. Altieri, A. Castro-Tirado, E. Costa, M. Feroci, F. Frontera, T. Galama, J. Gorosabel, P. Groot, J. Heise, C. Kouveliotou, E. Palazzi, J. van Paradijs, L. Piro, and M. Kessler: 1999. *A&AS* **138**, 459–460.
- Hazard, C., D. C. Morton, R. Terlevich, and R. McMahon: 1984. *ApJ* **282**, 33–52.
- He, J. H. and P. S. Chen: 2004. *New Astronomy* **9**, 545–564.
- Heckman, T. M.: 1980. *A&A* **87**, 152–164.
- Heckman, T. M., C. Robert, C. Leitherer, D. R. Garnett, and F. van der Rydt: 1998. *ApJ* **503**, 646+.
- Helou, G., N. Y. Lu, M. W. Werner, S. Malhotra, and N. Silbermann: 2000. *ApJ* **532**, L21–L24.
- Hirashita, H. and L. K. Hunt: 2004. *A&A* **421**, 555–570.
- Houck, J. R., B. T. Soifer, G. Neugebauer, C. A. Beichman, H. H. Aumann, P. E. Clegg, F. C. Gillett, H. J. Habing, M. G. Hauser, F. J. Low, G. Miley, M. Rowan-Robinson, and R. G. Walker: 1984. *ApJ* **278**, L63–L66.
- Hunt, L. K., L. Vanzì, and T. X. Thuan: 2001. *A&A* **377**, 66–72.
- Hur, M., G. J. Stacey, J. A. Fischer, H. A. Smith, S. Unger, S. D. Lord, and M. J. Barlow: 1996. *Bulletin of the American Astronomical Society* **28**, 1392+.
- Hwang, C., K. Y. Lo, Y. Gao, R. A. Gruendl, and N. Y. Lu: 1999. *ApJ* **511**, L17–L20.
- Imanishi, M.: 2002. *ApJ* **569**, 44–53.
- Ivion, R. J., J. S. Dunlop, D. H. Hughes, E. N. Archibald, J. A. Stevens, W. S. Holland, E. I. Robson, S. A. Eales, S. Rawlings, A. Dey, and W. K. Gear: 1998. *ApJ* **494**, 211+.
- Jarrett, T. H., G. Helou, D. Van Buren, E. Valjavec, and J. J. Condon: 1999. *AJ* **118**, 2132–2147.
- Joseph, R. D.: 1999. *Ap&SS* **266**, 321–329.
- Kegel, W. H., T. Hertenstein, and A. Quirrenbach: 1999. *A&A* **351**, 472–476.
- Kennicutt, R. C.: 1998. *ARA&A* **36**, 189–232.
- Kewley, L. J., M. A. Dopita, R. S. Sutherland, C. A. Heisler, and J. Trevena: 2001. *ApJ* **556**, 121–140.

- Klaas, U., M. Haas, S. A. H. Müller, R. Chini, B. Schulz, I. Coulson, H. Hippelein, K. Wilke, M. Albrecht, and D. Lemke: 2001. *A&A* **379**, 823–844.
- Klaas, U., R. J. Laureijs, and J. Clavel: 1999. *ApJ* **512**, 157–161.
- Klaas, U. and H. J. Walker: 2002. *A&A* **391**, 911–915.
- Kleinmann, D. E. and F. J. Low: 1970a. *ApJ* **161**, L203+.
- Kleinmann, D. E. and F. J. Low: 1970b. *ApJ* **159**, L165+.
- Krause, O., U. Lisenfeld, D. Lemke, M. Haas, U. Klaas, and M. Stickle: 2003. *A&A* **402**, L1–L4.
- Kriss, G. A., A. F. Davidsen, W. Zheng, J. W. Kruk, and B. R. Espey: 1995. *ApJ* **454**, L7+.
- Kuraszkiewicz, J. K., B. J. Wilkes, E. J. Hooper, K. K. McLeod, K. Wood, J. Bjorkman, K. M. Delain, D. H. Hughes, M. S. Elvis, C. D. Impey, C. J. Lonsdale, M. A. Malkan, J. C. McDowell, and B. Whitney: 2003. *ApJ* **590**, 128–148.
- Laureijs, R. J., J. Acosta-Pulido, P. Abraham, U. Kinkel, U. Klaas, H. O. Castaneda, L. Cornwall, C. Gabriel, I. Heinrichsen, D. Lemke, G. Pelz, B. Schulz, and H. J. Walker: 1996. *A&A* **315**, L313–L316.
- Laurent, O., I. F. Mirabel, V. Charmandaris, P. Gallais, S. C. Madden, M. Sauvage, L. Vigroux, and C. Cesarsky: 2000. *A&A* **359**, 887–899.
- Laurent, O., I. F. Mirabel, V. Charmandaris, P. Gallais, L. Vigroux, and C. J. Cesarsky: 1999. In: *ESA SP-427: The Universe as Seen by ISO*. pp. 913+.
- Le Floch, E., V. Charmandaris, O. Laurent, I. F. Mirabel, P. Gallais, M. Sauvage, L. Vigroux, and C. Cesarsky: 2002. *A&A* **391**, 417–428.
- Le Floch, E., I. F. Mirabel, O. Laurent, V. Charmandaris, P. Gallais, M. Sauvage, L. Vigroux, and C. Cesarsky: 2001. *A&A* **367**, 487–497.
- Leech, K. J., R. Saxton, P. Barr, M. Santos-Lleo, E. Jiminez-Bailon, R. Diaz, K. Ghosh, and S. Soundararajaperumal: 2002. *Publications of the Astronomical Society of Australia* **19**, 152–154.
- Leger, A. and J. L. Puget: 1984. *A&A* **137**, L5–L8.
- Lemke, D., K. Mattila, K. Lehtinen, R. J. Laureijs, T. Liljeström, A. Leger, and U. Herbstmeier: 1998. *A&A* **331**, 742–748.
- Lipari, S.: 1994. *ApJ* **436**, 102–111.
- Lipari, S., R. Terlevich, R. J. Díaz, Y. Taniguchi, W. Zheng, Z. Tsvetanov, G. Carranza, and H. Dottori: 2003. *MNRAS* **340**, 289–303.
- Lonsdale Persson, C. J. and G. Helou: 1987. *ApJ* **314**, 513–524.
- Low, J. and D. E. Kleinmann: 1968. *AJ* **73**, 868+.
- Lu, N., G. Helou, M. W. Werner, H. L. Dinerstein, D. A. Dale, N. A. Silbermann, S. Malhotra, C. A. Beichman, and T. H. Jarrett: 2003. *ApJ* **588**, 199–217.
- Luhman, M. L., S. Satyapal, J. Fischer, M. G. Wolfire, P. Cox, S. D. Lord, H. A. Smith, G. J. Stacey, and S. J. Unger: 1998. *ApJ* **504**, L11+.
- Luhman, M. L., S. Satyapal, J. Fischer, M. G. Wolfire, E. Sturm, C. C. Dudley, D. Lutz, and R. Genzel: 2003. *ApJ* **594**, 758–775.
- Lutz, D., R. Genzel, E. Sturm, L. Tacconi, E. Wieprecht, T. Alexander, H. Netzer, A. Sternberg, A. F. M. Moorwood, R. A. E. Fosbury, K. Fricke, S. J. Wagner, A. Quirrenbach, H. Awaki, and K. Y. Lo: 2000a. *ApJ* **530**, 733–737.
- Lutz, D., D. Kunze, H. W. W. Spoon, and M. D. Thornley: 1998a. *A&A* **333**, L75–L78.
- Lutz, D., R. Maiolino, A. F. M. Moorwood, H. Netzer, S. J. Wagner, E. Sturm, and R. Genzel: 2002. *A&A* **396**, 439–448.
- Lutz, D., R. Maiolino, H. W. W. Spoon, and A. F. M. Moorwood: 2004a. *A&A* **418**, 465–473.

- Lutz, D., H. W. W. Spoon, D. Rigopoulou, A. F. M. Moorwood, and R. Genzel: 1998b. *ApJ* **505**, L103–L107.
- Lutz, D., E. Sturm, R. Genzel, A. F. M. . Moorwood, T. Alexander, H. Netzer, and A. Sternberg: 2000b. *ApJ* **536**, 697–709.
- Lutz, D., E. Sturm, R. Genzel, H. W. W. Spoon, A. F. M. Moorwood, H. Netzer, and A. Sternberg: 2003. *A&A* **409**, 867–878.
- Lutz, D., E. Sturm, R. Genzel, H. W. W. Spoon, and G. J. Stacey: 2004b. *A&A* **426**, L5–L8.
- Lutz, D., S. Veilleux, and R. Genzel: 1999. *ApJ* **517**, L13–L17.
- Müller, S. A. H., M. Haas, R. Siebenmorgen, U. Klaas, K. Meisenheimer, R. Chini, and M. Albrecht: 2004. *A&A* **426**, L29–L32.
- Madau, P., H. C. Ferguson, M. E. Dickinson, M. Giavalisco, C. C. Steidel, and A. Fruchter: 1996. *MNRAS* **283**, 1388–1404.
- Madden, S. C.: 2000. *New Astronomy Review* **44**, 249–256.
- Malhotra, S., G. Helou, G. Stacey, D. Hollenbach, S. Lord, C. A. Beichman, H. Dinerstein, D. A. Hunter, K. Y. Lo, N. Y. Lu, R. H. Rubin, N. Silbermann, H. A. Thronson, and M. W. Werner: 1997. *ApJ* **491**, L27+.
- Malhotra, S., M. Kaufman, D. Hollenbach, G. Helou, R. Rubin, J. Brauher, D. Dale, N. Y. Lu, S. D. Lord, A. Contursi, T. Jarrett, and D. Hunter: 1999. *Bulletin of the American Astronomical Society* **31**, 1455+.
- Malhotra, S., M. J. Kaufman, D. Hollenbach, G. Helou, R. H. Rubin, J. Brauher, D. Dale, N. Y. Lu, S. Lord, G. Stacey, A. Contursi, D. A. Hunter, and H. Dinerstein: 2001. *ApJ* **561**, 766–786.
- Manning, C. and H. Spinrad: 2001. *AJ* **122**, 113–120.
- Martins, L. P., S. M. Viegas, and R. Gruenwald: 2003. *ApJ* **587**, 562–570.
- Masegosa, J., I. Márquez, M. J. Sempere, and J. Cernicharo: 2001. In: *ESA SP-460: The Promise of the Herschel Space Observatory*. pp. 459+.
- Mattila, K., K. Lehtinen, and D. Lemke: 1999. *A&A* **342**, 643–654.
- Mattila, K., D. Lemke, L. K. Haikala, R. J. Laureijs, A. Leger, K. Lehtinen, C. Leinert, and P. G. Mezger: 1996. *A&A* **315**, L353–L356.
- Meisenheimer, K., M. Haas, S. A. H. Müller, R. Chini, U. Klaas, and D. Lemke: 2001. *A&A* **372**, 719–729.
- Metcalf, L., S. J. Steel, P. Barr, J. Clavel, M. Delaney, P. Gallais, R. J. Laureijs, K. Leech, B. McBreen, S. Ott, N. Smith, and L. Hanlon: 1996. *A&A* **315**, L105–L108.
- Mihos, J. C. and L. Hernquist: 1996. *ApJ* **464**, 641+.
- Mirabel, I. F. and O. Laurent: 1999. *Ap&SS* **269**, 349–355.
- Mirabel, I. F., O. Laurent, D. B. Sanders, M. Sauvage, M. Tagger, V. Charmandaris, L. Vigroux, P. Gallais, C. Cesarsky, and D. L. Block: 1999. *A&A* **341**, 667–674.
- Mirabel, I. F., L. Vigroux, V. Charmandaris, M. Sauvage, P. Gallais, D. Tran, C. Cesarsky, S. C. Madden, and P.-A. Duc: 1998. *A&A* **333**, L1–L4.
- Mochizuki, K. and T. Onaka: 2001. *A&A* **370**, 868–874.
- Moorwood, A. F. M.: 1999. In: *ESA SP-427: The Universe as Seen by ISO*. pp. 825+.
- Moorwood, A. F. M., D. Lutz, E. Oliva, A. Marconi, H. Netzer, R. Genzel, E. Sturm, and T. de Graauw: 1996. *A&A* **315**, L109–L112.
- Morel, T., A. Efstathiou, S. Serjeant, I. Márquez, J. Masegosa, P. Héraudeau, C. Surace, A. Verma, S. Oliver, M. Rowan-Robinson, I. Georgantopoulos, D. Farrah, D. M. Alexander, I. Pérez-Fournon, C. J. Willott, F. Cabrera-Guerra, E. A. Gonzalez-Solares, A. Cabrera-Lavers, J. I. Gonzalez-Serrano, P. Ciliegi, F. Pozzi, I. Matute, and H. Flores: 2001. *MNRAS* **327**, 1187–1192.

- Mouri, H., Y. Taniguchi, Y. Sato, and K. Kawara: 1998. *A&A* **334**, 482–488.
- Murphy, T. W., B. T. Soifer, K. Matthews, and L. Armus: 2001. *ApJ* **559**, 201–224.
- Negishi, T., T. Onaka, K.-W. Chan, and T. L. Roellig: 2001. *A&A* **375**, 566–578.
- Nenkova, M., Ž. Ivezić, and M. Elitzur: 2002. *ApJ* **570**, L9–L12.
- Nollenberg, J. G., E. D. Skillman, D. R. Garnett, and H. L. Dinerstein: 2002. *ApJ* **581**, 1002–1012.
- Odenwald, S., J. Newmark, and G. Smoot: 1998. *ApJ* **500**, 554–+.
- O’Halloran, B., L. Metcalfe, M. Delaney, B. McBreen, R. Laureijs, K. Leech, D. Watson, and L. Hanlon: 2000. *A&A* **360**, 871–877.
- O’Halloran, B., L. Metcalfe, B. McBreen, R. Laureijs, K. Leech, M. Delaney, D. Watson, and L. Hanlon: 2002. *ApJ* **575**, 747–754.
- Oliva, E., A. Marconi, and A. F. M. Moorwood: 1999. *A&A* **342**, 87–100.
- Orr, M. J. L. and I. W. A. Browne: 1982. *MNRAS* **200**, 1067–1080.
- Pérez García, A. M. and J. M. Rodríguez Espinosa: 1998. *Ap&SS* **263**, 103–106.
- Pérez García, A. M. and J. M. Rodríguez Espinosa: 2001. *ApJ* **557**, 39–53.
- Pérez García, A. M., J. M. Rodríguez Espinosa, and J. J. Fuensalida: 2000. *ApJ* **529**, 875–885.
- Pagani, L., J. Lequeux, D. Cesarsky, J. Donas, B. Milliard, L. Loinard, and M. Sauvage: 1999. *A&A* **351**, 447–458.
- Peeters, E., L. J. Allamandola, D. M. Hudgins, S. Hony, and A. G. G. M. Tielens: 2003. *ArXiv Astrophysics e-prints*.
- Peeters, E., H. W. W. Spoon, and A. G. G. M. Tielens: 2004. *ApJ* **613**, 986–1003.
- Peng, B., A. Kraus, T. P. Krichbaum, S. A. H. Müller, S. J. Qian, A. Quirrenbach, S. J. Wagner, A. Witzel, J. A. Zensus, C. Jin, and H. Bock: 2000. *A&A* **353**, 937–943.
- Perez Garcia, A. M., J. M. Rodriguez Espinosa, and A. E. Santolaya Rey: 1998. *ApJ* **500**, 685–+.
- Plante, S. and M. Sauvage: 2002. *AJ* **124**, 1995–2005.
- Polletta, M. and T. J. L. Courvoisier: 1999a. In: *ESA SP-427: The Universe as Seen by ISO*. pp. 953–+.
- Polletta, M. and T. J.-L. Courvoisier: 1999b. *A&A* **350**, 765–776.
- Polletta, M., T. J.-L. Courvoisier, E. J. Hooper, and B. J. Wilkes: 2000. *A&A* **362**, 75–96.
- Popescu, C. C. and R. J. Tuffs: 2003. *A&A* **410**, L21–L24.
- Popescu, C. C., R. J. Tuffs, N. D. Kylafis, and B. F. Madore: 2004. *A&A* **414**, 45–52.
- Popescu, C. C., R. J. Tuffs, H. J. Völk, D. Pierini, and B. F. Madore: 2002. *ApJ* **567**, 221–236.
- Prieto, M. A. and J. A. Acosta-Pulido: 2003. *ApJ* **583**, 689–694.
- Prieto, M. A., A. M. Pérez García, and J. M. Rodríguez Espinosa: 2001. *A&A* **377**, 60–65.
- Puget, J. L. and A. Leger: 1989. *ARA&A* **27**, 161–198.
- Radovich, M., J. Kahanpää, and D. Lemke: 2001. *A&A* **377**, 73–83.
- Radovich, M., U. Klaas, J. Acosta-Pulido, and D. Lemke: 1999. *A&A* **348**, 705–710.
- Rigopoulou, D., D. Kunze, D. Lutz, R. Genzel, and A. F. M. Moorwood: 2002. *A&A* **389**, 374–386.
- Rigopoulou, D., D. Lutz, R. Genzel, E. Egami, D. Kunze, E. Sturm, H. Feuchtgruber, S. Schaeidt, O. H. Bauer, A. Sternberg, H. Netzer, A. F. M. Moorwood, and T. de Graauw: 1996. *A&A* **315**, L125–L128.
- Rigopoulou, D., H. W. W. Spoon, R. Genzel, D. Lutz, A. F. M. Moorwood, and Q. D. Tran: 1999. *AJ* **118**, 2625–2645.

- Rocca-Volmerange, B. and M. Remazeilles: 2005. *A&A* **433**, 73–77.
- Rodriguez Espinosa, J. M. and A. M. Perez Garcia: 1997. *ApJ* **487**, L33+.
- Rodriguez Espinosa, J. M., A. M. Perez Garcia, D. Lemke, and K. Meisenheimer: 1996. *A&A* **315**, L129–L132.
- Roussel, H., M. Sauvage, L. Vigroux, and A. Bosma: 2001. *A&A* **372**, 427–437.
- Rush, B., M. A. Malkan, and L. Spinoglio: 1993. *ApJS* **89**, 1–33.
- Sanders, D. B.: 1999. *Ap&SS* **266**, 331–348.
- Sanders, D. B. and I. F. Mirabel: 1996. *ARA&A* **34**, 749+.
- Sanders, D. B., B. T. Soifer, J. H. Elias, G. Neugebauer, and K. Matthews: 1988. *ApJ* **328**, L35–L39.
- Sanei, M. and S. Satyapal: 2002. *Bulletin of the American Astronomical Society* **34**, 1294+.
- Santos-Lleó, M., J. Clavel, B. Schulz, B. Altieri, P. Barr, D. Alloin, P. Berlind, R. Bertram, D. M. Crenshaw, R. A. Edelson, U. Giveon, K. Horne, J. P. Huchra, S. Kaspi, G. A. Kriss, J. H. Krolik, M. A. Malkan, Y. F. Malkov, H. Netzer, P. T. O’Brien, B. M. Peterson, R. W. Pogge, V. I. Pronik, B.-C. Qian, G. A. Reichert, P. M. Rodríguez-Pascual, S. G. Sergeev, J. Tao, S. Tokarz, R. M. Wagner, W. Wamsteker, and B. J. Wilkes: 2001. *A&A* **369**, 57–64.
- Satyapal, S., R. M. Sambruna, and R. P. Dudik: 2004. *A&A* **414**, 825–838.
- Sauvage, M., J. Blommaert, F. Boulanger, C. J. Cesarsky, D. A. Cesarsky, F. X. Desert, D. Elbaz, P. Gallais, G. Joncas, L. Metcalfe, K. Okumura, S. Ott, R. Siebenmorgen, J. L. Starck, D. Tran, and L. Vigroux: 1996. *A&A* **315**, L89–L92.
- Sauvage, M. and T. X. Thuan: 1992. *ApJ* **396**, L69–L73.
- Schaerer, D., T. Contini, and M. Pindao: 1999. *A&AS* **136**, 35–52.
- Schaerer, D. and G. Stasińska: 1999. *A&A* **345**, L17–L21.
- Schulz, B., J. Clavel, B. Altieri, P. Barr, P. Claes, A. M. Heras, K. J. Leech, and A. Metcalfe, L. and Salama: 2000. In: *ESA SP-456: ISO Beyond the Peaks: The 2nd ISO Workshop on Analytical Spectroscopy*. pp. 245+.
- Sellgren, K.: 1984. *ApJ* **277**, 623–633.
- Shier, L. M., M. J. Rieke, and G. H. Rieke: 1996. *ApJ* **470**, 222+.
- Siebenmorgen, R. and A. Efstathiou: 2001. *A&A* **376**, L35–L38.
- Siebenmorgen, R., W. Freudling, E. Krügel, and M. Haas: 2004a. *A&A* **421**, 129–145.
- Siebenmorgen, R., E. Krügel, and R. Chini: 1999a. *A&A* **351**, 495–505.
- Siebenmorgen, R., E. Krügel, and R. J. Laureijs: 2001. *A&A* **377**, 735–744.
- Siebenmorgen, R., E. Krügel, and H. W. W. Spoon: 2004b. *A&A* **414**, 123–139.
- Siebenmorgen, R., E. Krügel, and V. Zota: 1999b. *A&A* **351**, 140–146.
- Siebenmorgen, R. and E. Kruegel: 1992. *A&A* **259**, 614–626.
- Silva, L., G. L. Granato, A. Bressan, and L. Danese: 1998. *ApJ* **509**, 103–117.
- Skinner, C. J., H. A. Smith, E. Sturm, M. J. Barlow, R. J. Cohen, and G. J. Stacey: 1997. *Nature* **386**, 472–474.
- Smith, B. J.: 1998. *ApJ* **500**, 181+.
- Soifer, B. T., G. Neugebauer, K. Matthews, E. Egami, E. E. Becklin, A. J. Weinberger, M. Ressler, M. W. Werner, A. S. Evans, N. Z. Scoville, J. A. Surace, and J. J. Condon: 2000. *AJ* **119**, 509–523.
- Soifer, B. T., G. Neugebauer, K. Matthews, E. Egami, A. J. Weinberger, M. Ressler, N. Z. Scoville, S. R. Stolovy, J. J. Condon, and E. E. Becklin: 2001. *AJ* **122**, 1213–1237.
- Solomon, P. M., D. Downes, S. J. E. Radford, and J. W. Barrett: 1997. *ApJ* **478**, 144+.
- Spinoglio, L., P. Andreani, and M. A. Malkan: 2002. *ApJ* **572**, 105–123.

- Spinoglio, L., M. A. Malkan, H. A. Smith, and J. Fischer: 2003. In: *ASP Conf. Ser. 290: Active Galactic Nuclei: From Central Engine to Host Galaxy*. pp. 557–+.
- Spinoglio, L., M. A. Malkan, H. A. Smith, E. González-Alfonso, and J. Fischer: 2005. *ApJ* **623**, 123–136.
- Spoon, H. W. W., J. V. Keane, A. G. G. M. Tielens, D. Lutz, and A. F. M. Moorwood: 2001. *A&A* **365**, L353–L356.
- Spoon, H. W. W., J. V. Keane, A. G. G. M. Tielens, D. Lutz, A. F. M. Moorwood, and O. Laurent: 2002. *A&A* **385**, 1022–1041.
- Spoon, H. W. W., J. Koornneef, A. F. M. Moorwood, D. Lutz, and A. G. G. M. Tielens: 2000. *A&A* **357**, 898–908.
- Spoon, H. W. W., A. F. M. Moorwood, D. Lutz, A. G. G. M. Tielens, R. Siebenmorgen, and J. V. Keane: 2004. *A&A* **414**, 873–883.
- Stevens, J. A., M. Amure, and W. K. Gear: 2005. *MNRAS* **357**, 361–380.
- Stickel, M., J. M. van der Hulst, J. H. van Gorkom, D. Schiminovich, and C. L. Carilli: 2004. *A&A* **415**, 95–102.
- Struck, C.: 1999. *Phys. Rep.* **321**, 1–137.
- Sturm, E., T. Alexander, D. Lutz, A. Sternberg, H. Netzer, and R. Genzel: 1999. *ApJ* **512**, 197–203.
- Sturm, E., D. Lutz, R. Genzel, A. Sternberg, E. Egami, D. Kunze, D. Rigopoulou, O. H. Bauer, H. Feuchtgruber, A. F. M. Moorwood, and T. de Graauw: 1996. *A&A* **315**, L133–L136.
- Sturm, E., D. Lutz, D. Tran, H. Feuchtgruber, R. Genzel, D. Kunze, A. F. M. Moorwood, and M. D. Thornley: 2000. *A&A* **358**, 481–493.
- Sturm, E., D. Lutz, A. Verma, H. Netzer, A. Sternberg, A. F. M. Moorwood, E. Oliva, and R. Genzel: 2002. *A&A* **393**, 821–841.
- Sugai, H. and M. A. Malkan: 2000. *ApJ* **529**, 219–223.
- Suter, J. P., V. Harvey, P. Cox, J. Fischer, S. D. Lord, G. J. Melnick, S. Satyapal, H. A. Smith, G. Stacey, V. Strel'nitski, and S. J. Unger: 1998. *Bulletin of the American Astronomical Society* **30**, 1383–+.
- Takagi, T., N. Arimoto, and H. Hanami: 2003. *MNRAS* **340**, 813–831.
- Takeuchi, T. T., H. Hirashita, T. T. Ishii, L. K. Hunt, and A. Ferrara: 2003. *MNRAS* **343**, 839–850.
- Taniguchi, Y., L. L. Cowie, Y. Sato, D. B. Sanders, K. Kawara, R. Joseph, H. Okuda, C. G. Wynn-Williams, T. Matsumoto, K. C. Chambers, K. Wakamatsu, F. X. Desert, Y. Sofue, and H. Matsuhara: 1997. *A&A* **328**, L9–L12.
- Thornley, M. D., N. M. F. Schreiber, D. Lutz, R. Genzel, H. W. W. Spoon, D. Kunze, and A. Sternberg: 2000. *ApJ* **539**, 641–657.
- Thuan, T. X., M. Sauvage, and S. Madden: 1999. *ApJ* **516**, 783–787.
- Tran, Q. D., D. Lutz, R. Genzel, D. Rigopoulou, H. W. W. Spoon, E. Sturm, M. Gerin, D. C. Hines, A. F. M. Moorwood, D. B. Sanders, N. Scoville, Y. Taniguchi, and M. Ward: 2001. *ApJ* **552**, 527–543.
- Trewhella, M., J. I. Davies, P. B. Alton, S. Bianchi, and B. F. Madore: 2000. *ApJ* **543**, 153–160.
- Uchida, K. I., K. Sellgren, and M. Werner: 1998. *ApJ* **493**, L109+.
- Unger, S. J., P. E. Clegg, G. J. Stacey, P. Cox, J. Fischer, M. Greenhouse, S. D. Lord, M. L. Luhman, S. Satyapal, H. A. Smith, L. Spinoglio, and M. Wolfire: 2000. *A&A* **355**, 885–890.
- Vacca, W. D., K. E. Johnson, and P. S. Conti: 2002. *AJ* **123**, 772–788.
- Valentijn, E. A. and P. P. van der Werf: 1999. *ApJ* **522**, L29–L33.
- van Bemmell, I. M., P. D. Barthel, and T. de Graauw: 2000. *A&A* **359**, 523–530.
- Vanzi, L. and M. Sauvage: 2004. *A&A* **415**, 509–520.

- Vastel, C., E. T. Polehampton, J.-P. Baluteau, B. M. Swinyard, E. Caux, and P. Cox: 2002. *ApJ* **581**, 315–324.
- Veilleux, S. and D. E. Osterbrock: 1987. *ApJS* **63**, 295–310.
- Veilleux, S., D. B. Sanders, and D.-C. Kim: 1997. *ApJ* **484**, 92–+.
- Verma, A., D. Lutz, E. Sturm, A. Sternberg, R. Genzel, and W. Vacca: 2003. *A&A* **403**, 829–846.
- Verma, A., M. Rowan-Robinson, R. McMahon, and A. E. Efstathiou: 2002. *MNRAS* **335**, 574–592.
- Verstraete, L., C. Pech, C. Moutou, K. Sellgren, C. M. Wright, M. Giard, A. Léger, R. Timmermann, and S. Drapatz: 2001. *A&A* **372**, 981–997.
- Verstraete, L., J. L. Puget, E. Falgarone, S. Drapatz, C. M. Wright, and R. Timmermann: 1996. *A&A* **315**, L337–L340.
- Vigroux, L.: 1997. In: *Extragalactic Astronomy in the Infrared*. pp. 63–+.
- Vigroux, L., H. Aussel, V. Charmandaris, C. Cesarsky, D. Elbaz, D. Fadda, O. Laurent, S. Madden, F. Mirabel, H. Roussel, and M. Sauvage: 2001. *Astrophysics and Space Science Supplement* **277**, 565–569.
- Vigroux, L., V. Charmandaris, P. Gallais, O. Laurent, S. C. Madden, I. F. Mirabel, H. Roussel, M. Sauvage, and D. Tran: 1999. In: *ESA SP-427: The Universe as Seen by ISO*. pp. 805–+.
- Vigroux, L., F. Mirabel, B. Altieri, F. Boulanger, C. Cesarsky, D. Cesarsky, A. Claret, C. Fransson, P. Gallais, D. Levine, S. Madden, K. Okumura, and D. Tran: 1996. *A&A* **315**, L93–L96.
- Voit, G. M.: 1992. *ApJ* **399**, 495–503.
- Voit, G. M., R. J. Weymann, and K. T. Korista: 1993. *ApJ* **413**, 95–109.
- Wilson, C. D., N. Scoville, S. C. Madden, and V. Charmandaris: 2000. *ApJ* **542**, 120–127.
- Wilson, C. D., N. Scoville, S. C. Madden, and V. Charmandaris: 2003. *ApJ* **599**, 1049–1066.
- Xu, C., Y. Gao, J. Mazzearella, N. Lu, J. W. Sulentic, and D. L. Domingue: 2000. *ApJ* **541**, 644–659.
- Xu, C., J. W. Sulentic, and R. Tuffs: 1999. *ApJ* **512**, 178–183.

